

**NUCLEAR DATA AND MEASUREMENTS SERIES**

**ANL/NDM-41**

**Energy-Averaged Neutron Cross Sections of  
Fast-Reactor Structural Materials**

by

A. Smith, R. McKnight, and D. Smith

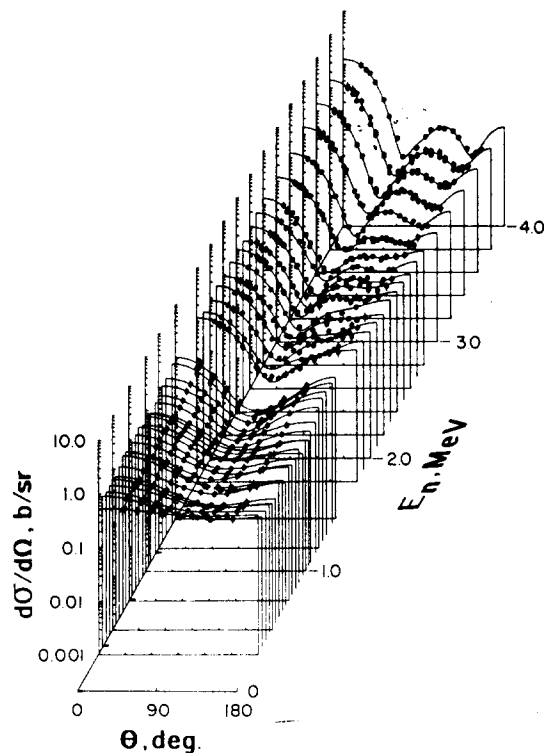
February 1978

**ARGONNE NATIONAL LABORATORY,  
ARGONNE, ILLINOIS 60439, U.S.A.**

# NUCLEAR DATA AND MEASUREMENTS SERIES

ANL/NDM-41  
ENERGY-AVERAGED NEUTRON CROSS SECTIONS OF FAST-  
REACTOR STRUCTURAL MATERIALS

by  
A. Smith, R. McKnight and D. Smith  
February 1978



U.S. AEC USERDA

ARGONNE NATIONAL LABORATORY,  
ARGONNE, ILLINOIS 60439, U.S.A.

The facilities of Argonne National Laboratory are owned by the United States Government. Under the terms of a contract (W-31-109-Eng-38) between the U. S. Atomic Energy Commission, Argonne Universities Association and The University of Chicago, the University employs the staff and operates the Laboratory in accordance with policies and programs formulated, approved and reviewed by the Association.

#### MEMBERS OF ARGONNE UNIVERSITIES ASSOCIATION

The University of Arizona  
Carnegie-Mellon University  
Case Western Reserve University  
The University of Chicago  
University of Cincinnati  
Illinois Institute of Technology  
University of Illinois  
Indiana University  
Iowa State University  
The University of Iowa

Kansas State University  
The University of Kansas  
Loyola University  
Marquette University  
Michigan State University  
The University of Michigan  
University of Minnesota  
University of Missouri  
Northwestern University  
University of Notre Dame

The Ohio State University  
Ohio University  
The Pennsylvania State University  
Purdue University  
Saint Louis University  
Southern Illinois University  
The University of Texas at Austin  
Washington University  
Wayne State University  
The University of Wisconsin

#### NOTICE

This report was prepared as an account of work sponsored by the United States Government. Neither the United States nor the United States Atomic Energy Commission, nor any of their employees, nor any of their contractors, subcontractors, or their employees, makes any warranty, express or implied, or assumes any legal liability or responsibility for the accuracy, completeness or usefulness of any information, apparatus, product or process disclosed, or represents that its use would not infringe privately-owned rights.

ANL/NDM-41  
ENERGY-AVERAGED NEUTRON CROSS SECTIONS OF FAST-  
REACTOR STRUCTURAL MATERIALS

by  
A. Smith, R. McKnight and D. Smith  
February 1978

In October 1977, the U. S. Energy Research and Development Agency (ERDA) was incorporated into the U. S. Department of Energy. The research and development functions of the former U. S. Atomic Energy Commission had previously been incorporated into ERDA in January 1975.

This document is the manuscript of an invited paper presented at the NEANDC/NEACRP Specialists' Meeting on Neutron Data of Structural Materials for Fast Reactors, Geel, Belgium, 5-8 December 1977.

Applied Physics Division  
Argonne National Laboratory  
9700 South Cass Avenue  
Argonne, Illinois 60439  
USA

\*

## NUCLEAR DATA AND MEASUREMENTS SERIES

The Nuclear Data and Measurements Series presents results of studies in the field of microscopic nuclear data. The primary objective is the dissemination of information in the comprehensive form required for nuclear technology applications. This Series is devoted to: a) measured microscopic nuclear parameters, b) experimental techniques and facilities employed in measurements, c) the analysis, correlation and interpretation of nuclear data, and d) the evaluation of nuclear data. Contributions to this Series are reviewed to assure technical competence and, unless otherwise stated, the contents can be formally referenced. This Series does not supplant formal journal publication but it does provide the more extensive information required for technological applications (e.g., tabulated numerical data) in a timely manner.

## TABLE OF CONTENTS

|  | Page |
|--|------|
| ABSTRACT. . . . .  | 1    |
| I.    INTRODUCTORY REMARKS . . . . .                                     | 1    |
| II.   TOTAL NEUTRON CROSS SECTIONS . . . . .                             | 2    |
| III.  NEUTRON ELASTIC AND NON-ELASTIC SCATTERING CROSS SECTIONS. . . . . | 5    |
| IV.  NEUTRON INELASTIC SCATTERING CROSS SECTIONS. . . . .                | 8    |
| V.   (n;p) CROSS SECTIONS . . . . .                                      | 12   |
| VI.  (n; $\alpha$ ) CROSS SECTIONS . . . . .                             | 16   |
| VII.  (n;n',p) CROSS SECTIONS. . . . .                                   | 18   |
| VIII. (n;n', $\alpha$ ) CROSS SECTIONS. . . . .                          | 20   |
| IX.  (n;2n') CROSS SECTIONS . . . . .                                    | 21   |
| X.   THEORETICAL APPLICATIONS . . . . .                                  | 22   |
| XI.  SYSTEM SENSITIVITIES . . . . .                                      | 26   |
| XII. GENERAL COMMENTS . . . . .  | 28   |
| REFERENCES. . . . .  | 30   |
| TABLES. . . . .  | 32   |
| FIGURES . . . . .  | 35   |

# ENERGY-AVERAGED NEUTRON CROSS SECTIONS OF FAST-REACTOR STRUCTURAL MATERIALS\*

by

A. Smith, R. McKnight, and D. Smith  
Argonne National Laboratory  
Argonne, Illinois, U.S.A.

## ABSTRACT

The status of energy-averaged cross sections of fast-reactor structural materials is outlined with emphasis on U. S. data programs in the neutron-energy range 1-10 MeV. Areas of outstanding accomplishment and significant uncertainty are noted with recommendations for future efforts. Attention is primarily given to the main constituents of stainless steel (e.g., Fe, Ni, and Cr) and, secondarily, to alternate structural materials (e.g., V, Ti, Nb, Mo, Zr). Generally, the mass regions of interest are  $A \sim 50-60$  and  $A \sim 90-100$ . Neutron total and elastic-scattering cross sections are discussed with the implication on the non-elastic-cross sections. Cross sections governing discrete-inelastic-neutron-energy transfers are examined in detail. Cross sections for the reactions  $(n;p)$ ,  $(n;n',p)$ ,  $(n;\alpha)$ ,  $(n;n',\alpha)$  and  $(n;2n')$  are reviewed in the context of fast-reactor performance and/or diagnostics. The primary orientation of the discussion is experimental with some additional attention to the applications of theory, the problems of evaluation and the data sensitivity of representative fast-reactor systems.

## I. INTRODUCTORY REMARKS

The intent is a qualitative outline of the energy-averaged nuclear data of structural materials over the energy range  $\sim 1-10$  MeV where explicitly relevant to Fast Breeding Reactor (FBR) concepts (1). The emphasis is on the status of contemporary U. S. programs but not to the complete exclusion of data available elsewhere. This discussion complements that of resonance phenomena (by Perey) and of radiative capture (by Allen) elsewhere in these proceedings. The discussion is limited to data important to FBR core-neutronics and/or FBR damage-dosimetry considerations. Peripheral FBR data needs (e.g., shielding, gamma production, etc.) are not addressed. Primary attention is given to the provision of structure data by experimental means. In this context the status is outlined with estimates of present and potential future uncertainties relevant to FBR needs and suggestions made as to productive future measurements. Primary attention is given to Fe, Cr, and Ni (i.e., constituents of stainless steel) and, secondarily, to the alternate structural materials near  $A \sim 50$  and  $A \sim 100$  (e.g., V, Ti, Co, Nb, Mo, and Zr). The reaction types: total cross sections (Sec. II), elastic scattering (Sec. III),  $(n;n')$  processes (Sec. IV),  $(n;p)$  cross sections (Sec. V),  $(n;\alpha)$  cross sections (Sec. VI),  $(n;n',p)$  processes (Sec. VII),  $(n;n',\alpha)$

\*This work supported by the U. S. Department of Energy.

processes (Sec. VIII), and  $(n;2n')$  cross sections (Sec. IX) are treated in a relatively independent manner thus those readers with special interests can directly refer to the relevant sections. Illustrations of the capabilities and limitations of theory in extrapolating and interpolating measured data are cited in Sec. X. The discussion is placed in the proper context of some FBR structure-data sensitivities in Sec. XI. Throughout, problems associated with the intermediate evaluation steps between microscopic data and integral use are noted. Finally, some general comments are made in Sec. XII.

A number of subjective, and even provocative, views are expressed in the hope that they will stimulate considerations that will result in an improved FBR-structure-data base.

## II. TOTAL NEUTRON CROSS SECTIONS

*A first "benchmark" test of an evaluated data set is a comparison of broad-resolution total cross sections with the energy-average of the evaluated file.*

The measured broad-resolution cross sections must be of sufficient scope for a representative average and the experimental uncertainties should be  $\sim 1\%$ . Such broad-resolution measurements are not trivial but have recently been employed to test both evaluations and high-resolution experimental results (2). The consequences are not entirely encouraging as illustrated by the following examples.

Results of broad-resolution ( $\sim 100$  keV) measurements of the iron total cross sections were not particularly consistent with the comparable energy average of ENDF-IV values as illustrated in Fig. 1 (2). From 1.5-3 MeV the average of the evaluated magnitudes is as much as 6% lower than the measured values and generally 3-5% lower. The evaluation was by competent personnel and probably correctly summarizes the available experimental information. The discrepancy is reflected in the partial cross sections and, in this instance, contributes to evaluated iron elastic scattering cross sections that are  $\sim 10\%$  lower than indicated by recent measurements (see Secs. III and IV). The indicated increase in iron elastic scattering has an impact on FBR core parameters - typically  $\sim +0.05\%$  in  $k_{eff}$ ,  $\sim -0.03\%$  in breeding ratio, and  $\sim -0.04\%$  in 238/249 fission ratio. These are small but significant changes and in a direction tending to resolve outstanding discrepancies between measured and calculated core parameters. The source of the above discrepancy could not be exactly identified. However, it is in a region where the iron total cross section is characterized by large and overlapping resonance structure. Measurements have often sought to resolve the structure and, in doing so, have employed relatively thick samples with some abandon. Even so, the experimental resolution was short of the inherent fluctuations with consequent shelf-shielding and too small average-cross-section magnitudes. The effect is most pronounced between  $\sim 1.5-3.0$  MeV where the disparity between resolution and structure has been largest. This explanation is supported by the recent very-high resolution results of Harvey et al. (3). The resolution of these recent measurements approaches that of the inherent structure and their energy average agrees to within  $\sim 1\%$  with the results of the broad-resolution measurements as illustrated in Fig. 1. Moreover, if there is any continuing

discrepancy it is toward too small high-resolution results as would be expected from the still incomplete resolution (4). Uncertainties in iron total cross sections should be greatly reduced in a future evaluation. It is not necessarily so for other nuclides.

An acute example of the discrepancy between measured energy-averaged and averaged high-resolution total cross sections is illustrated by the case of titanium shown in Fig. 2 (2,5). The high resolutions employed in the reported measurements (6) fell short of fully defining the physical structure and the samples involved were very thick. As a consequence the average magnitude of the fine-resolution cross sections falls 10-20% below the energy-averaged values measured with attention to resonance perturbation effects (2). The discrepancies are largest at the lower energies where the inherent structure is more pronounced and decrease as the energy increases and the structure broadens and overlaps. The implications on the non-elastic cross section can be considerable. Indeed, at some energies the fine-resolution total cross sections and the elastic-scattering cross sections (see Sec. III) imply negative inelastic scattering cross sections where they are known to be positive and large. As a consequence of this titanium discrepancy the proposed ENDF-V evaluation relies upon total-cross-section magnitudes determined from the broad-resolution measurements and uses the fine-resolution results only to obtain a qualitative indication of structure.

Measured broad- and high-resolution total cross sections of Ni-60 are in good agreement as illustrated in Fig. 3 (4,7). This is entirely consistent with the above discrepancies apparently rooted in self-shielding effects. The limited isotopic availability severely restricted sample size, and as a consequence self-shielding perturbations are small in both types of measurements and the results agree to within  $\sim 1\%$  on the average despite resolutions that fall short of the true structure. Unfortunately, calculations show both Ni-60 results to be too small by several percent. This was not experimentally verified as it was not practical to "chop" the unique sample into pieces.

The above and similar comparisons involving measured and evaluated data from a diversity of sources, suggest that:

*The energy-averaged magnitudes of total cross sections in the fluctuating structural region are generally not known to high precision,*

with uncertainties of  $\sim 10\%$  in some cases. These uncertainties can be magnified by a factor of two in the non-elastic and partial cross sections. Thus it is suggested that:

*All high resolution and fluctuating total cross sections in the MeV region should be verified with broad resolution measurements free of self-shielding perturbations.*

More generally, resonance structure in the MeV region should be viewed in the context of FBR calculational needs. It is good contemporary practice to employ a  $\sim 2000$  fine-group structure in FBR calculations (e.g., MC<sup>2</sup>-II, Ref. 8). This implies group widths of approximately 5 keV at 1 MeV, 15 keV at 2 MeV and 30 keV at 4 MeV. Thus the FBR core calculational group structure is to intermediate energy resolutions well below those sought in some measurements. Discrete-ordinate Monte-Carlo methods (e.g., VIM, Ref. 9) have the potential

for finer resolutions but in practice are inhibited by calculational costs. Effective and more detailed group calculations could potentially be made if suitable resonance descriptions were available. However, contemporary ENDF practice is deficient in resonance description even at energies less than 1 MeV and there remains the problem of deriving resonance parameters from experimental results in the complex few MeV region. Thus:

*The wisdom of data determinations to resolutions well beyond the capability of near term FBR calculational methods should be critically examined.*

Major attention to detailed resonance structure should probably focus on energies below those of the present discussion (e.g., See the companion paper by Perey.)

It is common ENDF evaluation practice at energies of  $\gtrsim 1$  MeV to reflect all total-cross-section resonance structure in the elastic-scattering channel, with the often very large contribution of other channels following a relatively slow energy dependence. This is obviously a physically dubious procedure that, in acute cases, can imply a non-unitary S-matrix. The consequences of this evaluation procedure on FBR calculations apparently have not been explored in detail. They may become significant as the inappropriate evaluation obviously biases the energy transfer process with consequent effects on the determinations of heterogeneity corrections and small sample perturbations. Moreover, some new test concepts (e.g., SAREF) involve massive components of structural sections. These considerations suggest that:

*Attention should be given to the concurrent determination of the total and partial cross sections of structural materials with modest but equivalent resolutions sufficient to define an internally consistent evaluated data set to the resolutions employed in contemporary calculational practice.*

This objective is within present measurement capability.

The implications of the above uncertainties in the MeV energy-averaged total cross sections on model interpretation can be significant as the total cross section is one of the few explicitly calculable parameters. A characteristic difficulty in the  $A \sim 50$  region is the inability of the model calculations to reproduce the observed minimum of the total cross section near 1 MeV. The discrepancy is 5-10% or more in many instances and generally of the same nature as observed between careful energy-averaged measurements and the average of some thick-sample high-resolution values as illustrated above.

*Before dealing with the complexities of energy-averaged models (e.g., vibrational coupling, etc.) attention should be given to the validity of the experimental energy-averaged total cross sections that are so much of their foundation.*

The above remarks are generally relevant to the 1-5 MeV energy region. There are also a number of glaring total cross section shortcomings at the lower energies discussed in the companion paper (Perey). Above 5 MeV very few total cross sections are generally consistent to better than 2-4%. In view of the supposed simplicity of the measurements:

*The general total cross section situation is an embarrassment.*

The above issues are not limited to FBR structural materials but also extend to the coolant sodium. The inelastic cross sections of sodium as given in ENDF-IV are probably, on the average, 5-10% too large over wide energy ranges (10). The problem appears partly associated with an uncertain reference standard. There is a school of thought that holds that the sodium elastic scattering cross sections of ENDF-IV are also too large. It seems that something is significantly wrong with the partials, totals, or both.

### III. NEUTRON ELASTIC AND NON-ELASTIC SCATTERING CROSS SECTIONS

The key physical concept in the study of elastic scattering from FBR structural materials is "fluctuations." Generally, the nuclides are even and near the peak of the  $\ell_0$  strength function. As a consequence the fluctuations in the elastic scattering channel are very large well into the many MeV region. Meaningful measurements must be of an angle/energy scope that will provide a reasonable sampling of these fluctuations. Single distributions, no matter how precise, do not properly represent the energy-averaged behavior and may, indeed, be deceptive. For reasonable definition of elastic neutron scattering from fast-reactor structural materials:

*It is essential that measurements be of sufficient energy/angle scope to reasonably sample the statistical behavior of the large fluctuations.*

For the primary fast-reactor structural materials ( $A \sim 50$ ) this requirement extends to at least 5 MeV. Few measurement programs meet this objective. The above wisdom can now be explicitly illustrated at the lower limit of the MeV region using the excellent high-resolution results described in the companion paper (Perey et al.). These high-resolution values and Monte-Carlo techniques have been used to computer-simulate a broad-resolution measurement with results such as illustrated in Fig. 4 (4). The results of this representative 30-keV-resolution "experiment" are very much dependent upon exact energy scale and resolution. Clearly, any single one of these distributions has little meaning. A far larger sample and broader-average resolutions are called for. Even then attention must be given to sample size to assure that correction factors, that can only be crudely estimated, are kept small. It is noted that the same simulation showed fluctuations of smaller magnitude in the companion inelastic-scattering cross sections. Ignorance of fluctuations has led to problems in evaluation and interpretation of elastic scattering from structural materials well into the MeV range. The fluctuations are less acute in the region of secondary FBR interest near  $A \sim 100$  but even there they cannot be ignored at the lower energies.

The status of elastic neutron scattering from the primary FBR structured materials: iron, nickel, and chromium, is outlined as follows:

Iron. The status is summarized in Fig. 5. Below 4 MeV there is a wealth of information that well defines the elastic cross sections with an energy resolution consistent with intermediate resonance structure and provides the angle-integrated cross section to  $\sim 5\%$  from 1-4 MeV. The results are less definitive and less consistent above 4 MeV suggesting an angle-integrated accuracy of 10-15% from 4-10 MeV.

*All FBR requests for differential elastic scattering cross sections of iron are satisfied over the range 1-4 MeV.*

A possible exception is a 5% request for values at "several peaks and valleys" with 1% energy resolution. That request can be fully met if the "several" is defined and the request is not relevant to FBR core physics.

*Requests for iron differential elastic scattering data above 4 MeV are generally not satisfied.*

Some of these are for 5% accuracies that certainly have not been achieved. Others are for 10% accuracies which are only marginally approached. This is particularly true in the range 4-6 MeV where Wick's Limit is not of much assistance.

The above results imply a non-elastic cross section and thus a total inelastic-scattering cross section that approaches some expressed data requirements.

Nickel. The knowledge of elastic scattering from nickel is analogous to that from iron as illustrated in Fig. 6. The understanding is enhanced by some detailed studies of scattering from the prominent isotope Ni-60 with the results shown in Fig. 7 (4). These recent Ni-60 values are indicative of contemporary capability. The results are of good detail and scope. The overall uncertainty in the individual points is  $\sim 5\%$  and the reproducibility of the measurements is 2-3%. In view of these results the differential and angle-integrated elastic scattering cross sections of Ni are known to  $\sim 5\%$  with a resolution of intermediate structure from 1-4 MeV. Thus:

*All FBR requests for nickel elastic-scattering cross sections are satisfied from 1-4 MeV.*

Above 4 MeV the elastic cross sections are known to  $\sim 10-15\%$  with the additional uncertainties due to fluctuations in the 4-6 MeV region. Thus

*Approximately half the requests for nickel elastic scattering data in the range 4-10 MeV are satisfied.*

Accuracies of  $\sim 5-10\%$  have not been achieved in this energy range. Measurements can provide  $\sim 5\%$  accuracies which will define the non-elastic, and thus the total inelastic, cross sections to  $\sim 10\%$  above 4 MeV and therefore be responsive to needs for nickel inelastic scattering data.

Chromium. Chromium elastic scattering is not as well known as that of iron and nickel. This became very obvious in the preparation of this review, and recourse was made to unpublished files dated from 10-15 years ago (11). Their contents apparently are even now a major source of data at the lower energies. The generally unsatisfactory situation is outlined in Fig. 8. With the possible exception of  $E_n \sim 1.5$  MeV, the elastic-scattering cross sections are not known to 5%. Above 4 MeV the accuracy of the data base is no better than  $\sim 10-15\%$ . Between 1.5-4 MeV the fluctuations are strong and there is no assurance that the limited available information is representative of the energy-averaged behavior much less the intermediate structure. Thus:

*Requirements for chromium elastic scattering data to accuracies of  $\sim 10\%$  are not generally met and future measurements should give particular attention to the process from 1-10 MeV.*

At energies above 5 MeV 20% accuracy requirements are met but those at the  $\sim 10\%$  level are in doubt. This lack of knowledge is reflected in the non-elastic, and thus inelastic, cross sections. Shortcomings in the chromium inelastic scattering cross sections are a matter of concern.

There is minor FBR interest in the elastic scattering cross sections of some other structural materials in the  $A \sim 50$  region. They can be important in other applications, e.g., fusion systems. These cross sections are illustrated by:

Titanium. The elemental elastic-scattering-cross sections in the energy range of interest are outlined in Fig. 9. The definition is sufficient to provide angle-integrated values with intermediate energy resolutions of 50-100 keV to  $\sim 5\%$  from 1-4 MeV and to  $\sim 10-20\%$  from 4-10 MeV. Coupled with the total cross sections noted above, the energy-averaged non-elastic cross sections are defined to  $\sim 20\%$  from 1-4 MeV and  $\sim 10-20\%$  from 4-10 MeV. As a consequence the total inelastic-scattering cross sections are known to similar accuracies. Below 4 MeV this result is consistent with the directly measured inelastic-scattering cross sections.

Vanadium. The status of elastic-scattering cross sections of vanadium is analogous to that of titanium but, if anything, of better quality as illustrated in Fig. 10. Expressed FBR interest in these cross sections is only to the 10% accuracy level and broad resolution. Thus:

*Requests for vanadium elastic scattering cross sections are certainly met to 4 MeV*

and partially so to 10 MeV. The implied non-elastic and inelastic-scattering cross sections are defined with accuracies that are significant in the context of modest requirements for inelastic-scattering data.

Nuclides near  $A \sim 100$  are not of primary FBR-structural interest. They are relevant to FBR fission-product effects and to other nuclear-energy concepts. Fluctuations remain a problem only at the low-MeV energies thus a more-limited data base reasonably defines the energy-averaged behavior of the elastic scattering throughout the MeV region. The relatively good status of elastic scattering in this region is illustrated by niobium (Fig. 11), molybdenum (Fig. 12), and zirconium (Fig. 13).

*Experimental results coupled with a modest theoretical interpolation satisfy FBR needs for structural elastic scattering data in the mass/energy region  $A \sim 100/1-10$  MeV.*

The requested elastic-scattering accuracies are modest ( $>10\%$ ) and can be reasonably met from existing information excepting only some isotopic elastic-scattering cross sections that appear to be special cases (e.g., isotopes of zirconium).

#### IV. NEUTRON INELASTIC SCATTERING CROSS SECTIONS

Inelastic neutron scattering from the FBR structural materials is characterized by strong energy-dependent fluctuations well into the MeV region.  $(n;n')$  or  $(n;n',\gamma)$  measurements at isolated energies and/or angles will not reliably determine cross sections to accuracies of 5-10% and, indeed, may lead to deceptive results. At energies well above the region of fluctuation the prominent inelastic processes remain anisotropic due to the onset of significant direct-reaction processes.

*Measurement of the inelastic scattering process in primary FBR structural materials must be of an energy and angle scope sufficient to define the angular distributions in the context of intermediate structure.*

Very few measurements have reasonably achieved this goal.

The nuclides of primary interest (i.e., Fe, Ni and Cr) are largely composed of even isotopes, have inelastic neutron scattering thresholds at  $\sim 1$  MeV, and inelastic scattering cross sections to energies of  $\sim 3$  MeV that are dominated by contributions from 2(+) and 4(+)-2(+)-0(+) vibrational structures. These structures are not demanding of experimental scattered-neutron resolution and lead to relatively unambiguous interpretations of  $(n;n',\gamma)$  results. It is potentially possible to quantitatively correlate fine and intermediate resolution  $(n;n')$  and  $(n;n',\gamma)$  results to  $\sim 2$  MeV. This has been achieved using results of recent studies of inelastic neutron scattering from Fe-56. High resolution results (outlined in the companion paper; Perey) define the cross section for the excitation of the 847 keV state in Fe-56 to 2 MeV as illustrated in Fig. 14. These results are in good agreement with those obtained in recent intermediate resolution  $(n;n')$  and  $(n;n',\gamma)$  measurements (24). This agreement was achieved only with careful attention to angular, geometric, and energy-resolution effects. Such comparisons are not always that encouraging. For example, the same intermediate resolution  $(n;n')$  and  $(n;n',\gamma)$  results noted in Fig. 14 are compared with an equivalent average of ENDF-IV in Fig. 15. Below  $\sim 1.5$  MeV there is a systematic tendency for the ENDF-IV values to be larger by 5-10% and that difference exceeds the requested FBR accuracies for this particular cross section. The discrepancy appears associated with the angular distribution of the emitted gamma-rays. In transitions of this type,  $P_4$  components of the gamma-ray distribution are significant and thus:

*The common practice of making  $(n;n',\gamma)$  measurements at a  $P_2$  node of the gamma-ray distribution can systematically distort the angle-integrated cross sections*

by amounts equivalent to or exceeding the requested FBR accuracy requirements.

The above iron example of complementary fine and broad resolution  $(n;n')$  and  $(n;n',\gamma)$  results is exceptional and generally not representative of the situation in Ni, Cr, and other  $A \sim 50$  nuclides. Near threshold the inelastic processes are similar thus:

*Complementary fine and intermediate resolution  $(n;n')$  and  $(n;n',\gamma)$  measurement programs should be initiated defining the relative inelastic scattering cross sections near  $A \sim 50$  from threshold to at least the onset of the second inelastic channel.*

$(n;n',\gamma)$  techniques are especially useful near threshold where the inelastically-scattered neutron is of very low energy and difficult to directly measure. Attention should be given to angular distributions and relative flux normalization with the objective of the relative inelastic cross sections to 5% accuracies. The above suggestion will provide detailed and accurate information from threshold to threshold  $\sim 500$  keV, meeting FBR needs in this energy region. These procedures are relatively free from uncertainties associated with the normalization of  $(n;n',\gamma)$  results at higher energies and in regions of heavier mass.

The above remarks are generally confined to the  $A \sim 50$  region and to energies of  $\sim 2$  MeV, i.e., to the lower-energy scope of this paper. With higher energies and heavier masses the  $(n;n',\gamma)$  technique becomes increasingly difficult and primary reliance is placed upon direct  $(n;n')$  detection techniques. Those techniques are capable of resolving the structure to  $\sim 5$  MeV with cross sections determined relative to the basic  $H(n;n)$  standard to accuracies of  $\sim 5\%$ . The quality of the result is generally related to the degree of effort and the techniques have not been fully exploited in the structural-material region. The broad status of some of these higher-energy inelastic processes is illustrated in the following paragraphs.

Iron (4). The status of iron  $(n;n')$  cross sections above the second inelastic threshold ( $\sim 2.08$  MeV) is outlined in Fig. 16. The prominent feature is the excitation of the first  $2+$  (847 keV) state. Recent relatively detailed measurements define this excitation function to 5-10% to 4 MeV (4) and to lesser accuracies to 10 MeV (12,13). Contributions from higher lying states are not nearly as well known but are generally small below 3 MeV. The number of such contributions rapidly increases above 3 MeV and the respective cross sections are increasingly uncertain. The cumulative sum of these higher-energy components can be large leading to overall uncertainties in the iron total-inelastic-scattering cross section of at least 10-15% above 4 MeV. This is illustrated in Fig. 17 which compares the cumulative sum of the discrete excitation cross sections of Figs. 16 with the total inelastic scattering cross section as given in ENDF-IV. From 2-3 MeV the present estimates are in good agreement with ENDF-IV. That is not particularly surprising as some of the same input data used in Fig. 16 was also involved in the evaluation. Above 3 MeV the results of Fig. 17 suggest that the total inelastic scattering cross section of iron is  $\sim 10\%$  lower than given in ENDF-IV and the relative changes in the transfer matrix may be even larger. Above about 5 MeV the inelastic cross section is largely determined by the non-elastic cross section and that is uncertain by at least 10-15% as noted above. Thus a reasonable summary-estimate is:

*Uncertainties in the iron inelastic-scattering cross section for intermediate resolutions are 5-7% (threshold to 2 MeV), 7-10% (2-4 MeV) and 10-15% above 4 MeV.*

This implies that:

*FBR requests for iron inelastic scattering data are nearly met below 2 MeV, only partially satisfied to 4 MeV and generally not met at higher energies.*

There is no obstacle to achieving iron-inelastic-scattering accuracies in the 5-7% range to  $\sim 5$  MeV and determining the non-elastic (i.e., total inelastic) cross section to 7-10% accuracies from 5-10 MeV. Excepting the detailed elements of the transfer matrix:

*All FBR requests for iron inelastic scattering cross sections could be satisfied in the near future using conventional and available techniques.*

The above comments, together with those of Sec. II (above), imply that the elastic scattering cross sections of iron are larger than given in ENDF-IV by 10-20% from  $\sim 1.5$ -3 MeV. These are embarrassingly large uncertainties.

Nickel (14). The status of elemental nickel ( $n;n'$ ) cross sections is outlined in Fig. 18. The situation is similar to that of iron but complicated by the presence of two prominent and several minor isotopes which puts more demand on experimental resolution. Moreover, this reaction has not received the attention given to the iron ( $n;n'$ ) process and, as a consequence, it is not as well known. Below 4 MeV the cross sections are known to  $\sim 10$ -12% uncertainties with resolutions sufficient to resolve broad structure. Above 4 MeV the non-elastic cross section is known to  $\sim 10$ -15%. Some discrete excitation functions are better known (notably those of Ni-60) and the cross sections for the excitation of the continuum are reasonably defined. This suggests an ( $n;n'$ ) cross section uncertainty of  $\sim 15$ -18% from 4-10 MeV.

*The available results satisfy all FBR Ni emission cross section needs, marginally satisfy Ni ( $n;n'$ ) 10% accuracy needs to 4 MeV but not above and fall short of Ni ( $n;n'$ ) needs to 5-10% accuracies.*

The latter will probably not be achieved without individual attention to each of the two prominent isotopes Ni-58 and Ni-60. Such isotopic measurements can provide the requisite accuracies and detail as illustrated by the results of Fig. 19 (4,15). They are largely the result of very recent measurements specifically designed to achieve the FBR goal of  $\sim 5\%$  accuracies with intermediate resolution and illustrate what can be done in the wider scope of FBR structural materials. Similar results for the companion isotope, Ni-58, are not available and even these Ni-60 values must be extended to both lower and higher energies.

*Satisfying FBR high-precision needs for nickel ( $n;n'$ ) cross sections will probably require explicit study of the Ni-58 and Ni-60 isotopes and isotopic samples will be needed.*

With the provision of suitable samples, all FBR needs for nickel ( $n;n'$ ) cross sections can be met using existing capability.

Chromium. The ( $n;n'$ ) process in chromium should be similar to that in nickel but with enhanced fluctuations requiring particularly detailed measurements below  $\sim 5$  MeV. Such measurements have not been made and even the non-elastic cross section is poorly known (see above). This situation is reflected in the contemporary ENDF-IV file which is largely a theoretical construction involving some 40 states distributed between 1-7 MeV. Such theoretical constructions can be uncertain by 15-20% in this mass-energy region particularly where the excitation is dominated by a prominent  $2+$  vibrational configuration

as in this case. Thus the chromium (n;n') cross sections are the most uncertain of those of primary FBR interest.

*FBR needs for chromium (n;n') and emission cross sections to  $\sim 10\%$  accuracies are not met,*

and even a  $\sim 20\%$  goal is only marginally achieved.

*Attention should be given to chromium (n;n') cross sections, particularly at energies of  $\sim 5$  MeV, with resolutions sufficient to resolve intermediate structure.*

If Cr-50, 52, and 53 separated samples can be made available accuracies of  $\sim 5\%$  can be achieved as illustrated by the above Ni-60 results. Concurrently the non-elastic cross sections will be determined to  $\sim 10\%$ . The consequence will be the resolution of one of the most outstanding uncertainties in the (n;n') cross sections of stainless steel.

Vanadium. The inelastic scattering cross sections are explicitly known to  $\sim 4$  MeV to accuracies of 10-15% and with resolutions sufficient to resolve broad intermediate structure as illustrated in Fig. 20 (19,20). The results are not as comprehensive above 4 MeV but the non-elastic, some discrete-excitation and the continuum-emission cross sections are reasonably known.

*Thus the 15% requests for vanadium (n;n') cross sections are certainly satisfied to 4 MeV and partially so to 10 MeV.*

Any further FBR-oriented measurements should give emphasis to energies above 5 MeV.

Titanium. Despite the fact that a number of isotopes contribute to the (n;n') process in titanium, the corresponding cross sections are reasonably known as illustrated in Fig. 21 (5,17,18). Below  $\sim 5$  MeV the uncertainties are in the range 5-10% and the measurements are detailed enough to follow intermediate structure. Above 5 MeV the non-elastic cross section is known to  $\sim 10\%$  (see above and the inelastic-neutron emission spectrum has been reasonably determined. This data base provides a good foundation for a recent evaluation (17) that meets all FBR needs in this area and, to a large extent, satisfies fusion-system requirements. Should additional accuracy be required at a future date it will probably be necessary to study the individual isotopic components, particularly Ti-46 and Ti-48.

Niobium. The (n;n') reaction in niobium is illustrative of FBR dosimetry interest in such processes in the region of isomerism near  $A \sim 100$ . Similar isomer-producing reactions are Rh-103 (n;n') and In-115 (n;n'). The applied need is for the activation cross sections of relatively long-lived isomers having relatively low-energy thresholds. Explicit determinations of the (n;n') cross sections, such as those of niobium illustrated in Fig. 22 (21) and of Rh-103 of Ref. 25, provide supporting information and are of direct applied interest in other contexts, e.g., fusion neutronics. At present

*FBR needs for In-115 and Rh-103 (n;n') activation cross sections are largely met. That is not so for Nb (n;n').*

The latter cross section will be particularly difficult to determine to the requested  $\sim 5\%$  accuracies.

Molybdenum. Recently there has been renewed FBR interest in the  $(n;n')$  cross sections of the molybdenum isotopes. It is not clear whether this interest stems from structural use of molybdenum or the prominent position of the isotopes in the fission-product yield distributions. The cross sections are largely due to contributions from the even isotopes where the experimental results are reasonably complete as illustrated by Mo-100 shown in Fig. 23 (22). Similar results are available for the other even isotopes. Thus:

*FBR needs for  $(n;n')$  cross sections of the molybdenum isotopes are essentially met to 4 MeV.*

Moreover, the cross sections are relatively smooth functions of energy, the non-elastic cross section is known to 15-20% to 8 MeV and theory can reasonably extrapolate and interpolate from the measured data to accuracies of  $\sim 20\%$ .

*All FBR needs for molybdenum  $(n;n')$  data are met to 10 MeV.*

This is particularly so as the requested accuracies are a modest 20% and thus within the theoretical capabilities as outlined in Sec. X and discussed elsewhere in these proceedings by La Grange.

Zirconium. The character of inelastic scattering from the zirconium isotopes is much like that from molybdenum. Unfortunately, knowledge of the processes in zirconium is largely confined to the isotopes Zr-90 and Zr-92 (i.e., almost 70% of the element) (23). These results are illustrated in Fig. 24. The general uncertainties are in the order of 10-15% below 4 MeV.

*Thus, fission-reactor requests for zirconium inelastic scattering cross sections are not generally met.*

The requests are for detailed isotopic information to 10% accuracies to 10 MeV. Such accuracies will require suitable isotopic samples for productive measurements and these are not generally available. The requested accuracy is beyond theoretical capability as discussed in Sec. X. In view of these practical and physical problems it is doubtful that these zirconium needs will soon be met.

## V. $(n;p)$ CROSS SECTIONS

$(n;p)$  reactions near  $A \sim 50$  are characterized by low-energy thresholds and cross sections that rise rapidly from threshold to relatively large values (e.g.,  $\sim 0.5b$ ). Their response in a U-235 fission-neutron spectrum is very often essentially saturated at an energy of 10 MeV. The primary FBR interest is in hydrogen production and in reactor dosimetry and, with a few exceptions (notably long-term burn-up indexes), below 10 MeV. The relevant  $(n;p)$  reactions frequently result in active products that can, in principle, be studied with relative ease (explicitly so in the cases of dosimetry cross sections). As a consequence it is a straightforward matter to provide the requisite microscopic data and, in many cases, the cross sections are very well known. Shortcomings in the data are usually traceable to the absence of a disciplined

engineering approach and to uncertainties associated with various flux standards (e.g., fission cross sections). Generally:

*All FBR requests for microscopic (n;p) data have been, or can be easily, met.*

Specific cases of outstanding interest are outlined below. The respective reaction Q-values and isotopic abundances are given in Table 1.

Iron. The Fe-54 and Fe-56 (n;p) reactions are of major FBR interest due to their contribution to hydrogen production in stainless steels and to their use as dosimetry monitors. The Fe-56 (n;p) reaction is very well known, particularly as the result of recent measurements that define the cross section from 10 MeV to the microbarn region near threshold (27). The detail and consistency of the available information is illustrated in Fig. 25. The recent values of Ref. 27 are relative to U-235 and U-238 fission cross sections with ratio accuracies of  $\sim 5\%$ . Thus

*FBR requirements for the Fe-56 (n;p) cross section are largely satisfied.*

The required accuracy is  $\sim 5\%$  and that appears to have been achieved from the present (n;p) data base. This good status suggests that:

*The Fe-56 (n;p) cross section be accepted as a secondary reaction standard.*

The cross section is well known, relatively free of fluctuations and does not change very rapidly above  $\sim 6$  MeV. Future studies of the Fe-56 (n;p) should emphasize the region below  $\sim 8$  MeV as that is the region of primary FBR response as illustrated in Fig. 26. In doing so attention should be given to precise energy scales (28).

The Fe-54 (n;p) cross section is not as well known as that of Fe-56 as illustrated in Fig. 27. However, recent measurements define the cross section values relative to U-235 and U-238 fission to accuracies of  $\sim 5-8\%$  from near threshold to 10 MeV. (27). These newer results are not consistent with ENDF-IV and there remains a significant discrepancy between calculated and measured integral responses. Despite the relatively low isotopic abundance, the Fe-54 contribution to elemental hydrogen production is significant as the cross section is  $\sim 5$  larger than that of Fe-56. Thus

*FBR results for Fe-54 (n;p) cross sections are probably satisfied to 10 MeV*

if the recent results are as accurate as stated. They were a part of a program that has proven reliable in other contexts. Dosimetry oriented interests in the Fe-54 (n;p) cross section are satisfied at  $E_n \sim 10$  MeV excepting a single demand for 5% accuracies. Any:

*Future Fe-54 (n;p) measurements should give attention to energies  $\sim 8$  MeV.*

This is the area of primary FBR sensitivity, as illustrated in Fig. 26, and a region where the existing experimental results are most discrepant. The Fe-57 (n;p) reaction is of little FBR interest. The isotope is only  $\sim 2\%$  abundant

and what is known of the cross section near 14 MeV indicates a value of  $\sim 50$  mb. The product half-life is too short ( $\sim 1.7$  m) for convenient dosimetry use.

The above indicates that

*FBR requests for the (n;p) cross sections of elemental iron are met to 10 MeV.*

Nickel (14). The primary concern is for the (n;p) cross sections of the prominent isotopes Ni-58 and Ni-60. Contributions from the other isotopes are small. The Ni-58 (n;p) cross sections are relatively well known as summarized in Fig. 28. The recent results of Smith and Meadows (27) define the cross section from the microbarn level near threshold to 10 MeV. Essentially all of the response-function in a U-235 fission neutron spectrum lies below 10 MeV. A conservative estimate of the cross-section uncertainty is  $\sim 10\%$  to 10 MeV or  $\sim 5\%$  if the reference fission cross sections of U-235 and U-238 employed in the work of Ref. 27 are obtained to 1-2% accuracy levels. These are very good accuracies that:

*Satisfy all requests for microscopic (n;p) cross sections of Ni-58 at  $E_n \leq 10$  MeV.*

Thus future measurements should probably give first emphasis to the standard problems of U-235 and U-238 fission cross sections. Even now

*The Ni-58 (n;p) cross section is sufficiently well known below 10 MeV to constitute a secondary reaction standard in itself.*

The Ni-60 (n;p) cross sections are not as well known as those of Ni-58, as illustrated in Fig. 29. However, the isotope is of modest abundance, the cross section is a factor of X 4-5 smaller than that of Ni-58 and there is no explicit FBR interest in the isotopic reaction. Structure effects above 10 MeV have been interpreted in terms of quasi-particle effects (30) but are not a factor at energies below 10 MeV where essentially all of the FBR response function is concentrated. The cross section is uncertain below 5 MeV, thus:

*Future measurements of the Ni-60 (n;p) cross section should emphasize the energy region below 5 MeV.*

This region is of most FBR interest in the context of both dosimetry and hydrogen-production.

In view of the above, it is concluded that:

*FBR needs for elemental nickel (n;p) cross sections are met.*

Requested accuracies are a modest 10% and the FBR response function is largely saturated before the more uncertain region  $>10$  MeV is reached.

Chromium. The primary interest is in the (n;p) reaction with the isotopes Cr-52 and -53. Both processes lead to active products with half-lives too short to make them of any dosimetry interest. All available experimental

information is at energies above 10 MeV but suggests a relatively large (n;p) cross section. Roy (31) estimates a fission-spectrum-average cross section of 0.8 mb. That is a relatively large value. At present:

*Requests for chromium (n;p) cross sections are not satisfied.*

The desired accuracies are a modest 10-20% and:

*Measurements should provide for FBR chromium (n;p) needs.*

These are feasible with properly chosen activation techniques.

Cobalt (32). Recent results of Smith and Meadows (33) indicate large changes in the (n;p) cross section of cobalt from that given in ENDF-IV as illustrated in Fig. 30. The cross section is now defined from near threshold to 10 MeV with 5-8% accuracy. This energy-range spans  $\sim 95\%$  of the response-function in a U-235 fission spectrum. These new microscopic results lead to a good ( $\sim 1\%$ ) agreement between calculated and measured integral-response in a fission neutron spectrum (34). They are further supported by the results of higher-energy integral tests (35). Thus:

*Requests for the Co-59 (n;p) cross section are satisfied to 10 MeV.*

The present data base probably meets essentially all fast reactor needs for this reaction which are primarily dosimetry oriented. Any possible future measurements should probably concentrate on the limited objective of verifying the results of Ref. 33.

Vanadium (19). Essentially all of the (n;p) cross section is due to the prominent isotope, V-51. The experimental data base is not particularly well defined as illustrated in Fig. 31. Theoretical extrapolation must be entirely relied upon for cross section values below 10 MeV. These calculations indicate a large and competing (n;n',p) cross section and, as a consequence, the proposed ENDF-V evaluation is markedly lower (below 12 MeV) than that of ENDF-IV which did not include the (n;n',p) component. There is no known FBR interest in these cross sections though vanadium is often mentioned in a fusion-system context.

Titanium (17). The (n;p) cross sections of Ti-46, -47, and -48 are of FBR dosimetry interest. The remaining isotopes (Ti-49 and -50) are of relatively low abundance, have small cross sections and they are of no identifiable FBR interest. Recent measurements by Smith, et al. (17) define the cross sections of the above three isotopes from near threshold to 10 MeV. These results were obtained relative to U-235 and U-238 fission cross sections with the ratio values known to  $\sim 5\%$  even near threshold where the cross sections are  $\sim 1$  mb. These results are outlined and compared with previously available data and with evaluations in Figs. 32, 33, and 34. Reasonable evaluation of these results (e.g., Refs. 17 and 36) provides energy dependent cross sections to 10 MeV with uncertainties of  $\sim 5\%$ . The FBR response function is essentially saturated at 10 MeV for the Ti-46 and -47 (n;p) reactions and nearly so for Ti-48. Moreover, the calculated cross sections averaged over the fission spectrum agree with the results of integral "benchmark" measurements to within  $\sim 10\%$  which is approximately the uncertainty associated with the integral result alone. It is concluded that:

*FBR requests for titanium (n;p) data may be satisfied.*

A possible exception is a 5% accuracy requirement set by one laboratory. In the latter case, the present data base may be sufficient if the reference fission standards are made available to the requested  $\sim 2\%$  uncertainty level.

There has been a recent FBR interest expressed in the (n;p) cross sections of the molybdenum isotopes. The motivation appears to be due to gas production as the isomer chains and half-lives make the processes unattractive dosimeters. Qualitatively, the significant isotopes appear to be Mo-92, -94, and -95 with minor contributions from the others. Only Mo-92 appears to have a significant (n;n',p) component. The available information appears limited to reactor-spectrum and 14 MeV results. That data may suffice for meeting the present and modest 20% requirements.

## VI. (n; $\alpha$ ) CROSS SECTIONS

The (n; $\alpha$ ) reaction products tend to be tightly bound with low (or even exothermic) thresholds and stable reaction products. The cross sections are relatively large at low energies and the  $\chi$  response in a U-235 fission spectrum is often nearly saturated at energies of  $\sim 10$  MeV. Thus:

*(n; $\alpha$ ) reactions are a primary mechanism for helium production in FBR systems.*

The respective cross sections are generally not well known. Thus:

*FBR requirements for (n; $\alpha$ ) cross sections generally are not met.*

The measurement of (n; $\alpha$ ) cross sections is complicated by the stability of many of the products and even where activation methods are feasible the experimental results are often discrepant by amounts that are large compared to such factors as the uncertainties in the reference standards. Experimental knowledge is largely limited to helium-production cross sections measured by particle detection at  $\sim 15$  MeV (38) or by mass spectrometric study of reactor-radiated samples (e.g., radiations in EBR-II) (39). The helium-production cross section is not the (n; $\alpha$ ) cross section above the (n;n', $\alpha$ ) threshold (e.g., at  $\sim 15$  MeV) but such cross sections, extrapolated with theory as outlined in Sec. X, are the major near-term mechanism for providing a number of (n; $\alpha$ ) cross sections.

*Means for improving the scope of helium-production measurements should be sought,*

particularly to provide information in the energy region of primary FBR interest ( $\sim 10$  MeV). Attention should be given to new technologies and/or increased source intensities that would make the existing helium production techniques more widely applicable.

The (n; $\alpha$ ) reactions of primary FBR interest and their associated isotopic abundances and reaction Q-values are outlined in Table 2. Each is specifically dealt with in the following paragraphs.

Iron. The primary interest is in the Fe-54 and -56 (n; $\alpha$ ) reactions. The fission-spectrum response is small ( $\sim 1$  mb) but the reactions are a major source of helium production in FBR systems due to the abundance of iron. The Fe-54 (n; $\alpha$ ) reaction can be effectively studied with activation techniques. Despite this, knowledge of these cross sections is limited to a few qualitative values below 5 MeV ( $\sim 10$  mb) and to results at  $E_n \geq 14$  MeV ( $\sim 100$  mb). Thus it is suggested that:

*The Fe-54 (n; $\alpha$ ) reaction be carefully measured from threshold to 10 MeV using activation techniques.*

Accuracies of 10-20% can be expected if isotopically separated targets are available. The Fe-56 (and Fe-57) (n; $\alpha$ ) reaction results in a stable nucleus thus the corresponding cross sections must be theoretically deduced from the limited helium-production results cited above. Such interpretation provides Fe-56(n; $\alpha$ ) cross sections in the range of FBR interest to accuracies of 20-40%. Thus, at present:

*FBR requirements for iron (n; $\alpha$ ) cross sections to accuracies of 10-20% have not been met.*

The above suggested Fe-54(n; $\alpha$ ) measurements would directly contribute to the definition of iron (n; $\alpha$ ) cross sections and would give confidence to theoretical extrapolation of Fe-56 helium-production results.

Nickel (14). The Ni-58 and Ni-60 (n; $\alpha$ ) reactions are of primary FBR concern and are poorly known. The Ni-58 contribution is probably the dominant factor. Current knowledge of the nickel (n; $\alpha$ ) cross section is largely obtained from theoretical extrapolation between measured helium-production cross sections at  $\sim 15$  MeV (38) and in an FBR reactor spectrum with an effective energy of  $\sim 1$  MeV. The (n; $\alpha$ ) cross section in the reactor spectrum is  $\sim 5$  mb (31), a relatively large value. The Fe-55 product of the Ni-58(n; $\alpha$ ) reaction decays entirely by electron capture. Modern low-energy-photon-detection techniques have the potential for quantitative measurement of this decay, and thus the Ni-58(n; $\alpha$ ) cross section, over a wide energy range.

*It is suggested that photon detection be used to determine the Fe-55 activity and thus the Ni-58(n; $\alpha$ ) cross section.*

The Ni-60(n; $\alpha$ ) cross section is even more uncertain than that of Ni-58 but theoretical extrapolation suggests a smaller FBR response (by a factor of  $\sim 4$ ). Combining the above, the elemental nickel (n; $\alpha$ ) cross section is  $\sim 100$  mb at 10 MeV with an uncertainty of 20-30%. Thus:

*FBR requirements for nickel (n; $\alpha$ ) cross sections to 10-20% accuracies have not been met.*

With improvements in helium-production measurement techniques, successful photon studies of the decay of Fe-55 and the application of best contemporary theory the near-term FBR goal of nickel (n; $\alpha$ ) cross sections to  $\sim 20\%$  accuracy is realistic. A 10%-accuracy objective is far more difficult and probably will demand major technological improvements.

Chromium. The Cr-50, -52, and -53 (n; $\alpha$ ) reactions are of interest. All of the reaction products are stable and there is no microscopic cross-section information available at energies of  $<14$  MeV. Estimated fission-spectrum-averaged cross section values are 0.7 mb (50), 0.07 mb (52) and 3.0 (53) (31). If these values are correct the Cr-53(n; $\alpha$ ) process is a major concern. Estimates of the elemental cross sections rely on theoretical extrapolation in a manner analogous to that employed in nickel and iron, above. The results are qualitative and thus:

*FBR requests for chromium (n; $\alpha$ ) cross sections are not met.*

Providing for FBR needs for chromium (n; $\alpha$ ) cross sections are probably the most difficult of the iron-nickel-chromium (n; $\alpha$ ) triad as there appears to be no alternative to the correlated use of direct-particle detection, helium-production measurement and theoretical-calculation techniques and all three have serious shortcomings.

Cobalt (32). The cobalt (n; $\alpha$ ) reaction is well known to above 10 MeV as illustrated in Fig. 35. In the region of FBR interest ( $\sim 10$  MeV) the cross section uncertainties are  $\sim 5-10\%$  and calculated and measured responses in a U-235 fission spectrum are consistent to the same accuracies. Thus:

*Knowledge of the Co(n; $\alpha$ ) reaction meets FBR needs.*

Those needs are primarily in the area of core and vessel dosimetry.

Vanadium (19). The contemporary status of the vanadium (n; $\alpha$ ) reaction is outlined in Fig. 36. This cross section is not of FBR interest but it illustrates the large discrepancies between results of some activation measurements of this type and the application of theory subsequently supported by experiments. A recent evaluation did not make use of the latest available data (40) and relied entirely upon theoretical extrapolation from 14 MeV to threshold. Subsequently available measured results verified this extrapolation in detail even to the small "bump" near 10 MeV. This illustration gives credibility to the theoretical extrapolations that will remain essential to the provision of the above iron, nickel and chromium (n; $\alpha$ ) cross sections.

Titanium (17). There is no expressed FBR interest in the (n; $\alpha$ ) cross sections of the titanium isotopes. This is fortunate as these cross sections below  $\sim 10$  MeV must be entirely deduced by theoretical extrapolation from the marginally-known 14 MeV region.

(n; $\alpha$ ) channels are open in the  $A \sim 100$  region but the process is severely inhibited by the barrier and of little FBR interest.

## VII. (n;n',p) CROSS SECTIONS

The number of (n;n',p) reactions with thresholds of  $\sim 10$  MeV in FBR structural materials is limited to those of Table 3. In the primary materials (Fe, Ni, and Cr) no threshold is less than 8 MeV and only in nickel are isotopes of major abundance involved. Some of the residual products are unstable and activation techniques can provide quantitative (n;n',p) cross sections. Thus far results have been confined to energies  $\sim 14$  MeV but, with care, the

technique could be extended into the region of  $(n;n',p)$  thresholds below 10 MeV. Hydrogen-production measurements using direct-particle detection provide information relative to the  $(n;n',p)$  reaction. The available experimental data, essentially all above 14 MeV, must be theoretically extrapolated to the lower energies of FBR interest using the calculational methods outlined in Sec. X. The resulting cross sections below 10 MeV are uncertain but they are qualitatively much smaller than the corresponding  $(n;p)$  cross sections. Thus:

*The  $(n;n',p)$  reaction does not significantly contribute to hydrogen production in FBR systems.*

There may be some potential interest in  $(n;n',p)$  reactions for FBR dosimetry despite the requisite corrections for the  $(n;d)$  contamination. However, only one such dosimetry application can be identified and then at much higher energies (15 MeV).

The above general comments are illustrated by the following explicit examples.

Iron. The only reaction with a threshold  $<10$  MeV is  $\text{Fe-54}(n;n',p)(E_{th} \sim 9 \text{ MeV})$ . The isotope is of minor abundance. The cross sections are not experimentally known below 10 MeV but even if they rise rapidly from threshold the contribution to overall FBR hydrogen production will be small. Moreover, there is no evidence in the companion and much larger  $(n;p)$  cross section for an abrupt increase in the  $(n;n',p)$  cross section near threshold.

Nickel (14). Both Ni-58 and Ni-60 isotopes contribute to the  $(n;n',p)$  process below 10 MeV with the former the dominant factor due to the lower threshold and larger abundance. The reaction in Ni-58 is qualitatively known from activation measurements at energies of  $\sim 14$  MeV. Theoretical extrapolation indicates that the cross section falls rapidly to threshold with a value of  $\sim 70$  mb at 10 MeV. The Ni-60 component is not well known but the threshold is almost 10 MeV. Thus the elemental nickel  $(n;n',p)$  cross section is a factor of X 5-10 smaller than the  $(n;p)$  cross section at energies  $\sim 10$  MeV and makes a minor contribution to hydrogen production in FBR systems. There is no evidence in the companion  $(n;p)$  cross sections for an anomalous behavior of the  $(n;n',p)$  reaction that would alter this conclusion. There is dosimetry interest in the Ni-58  $(n;n',p)$  reaction for burn-up assay purposes. The objective of 10% accuracy at 15 MeV has not been met but appears to be within contemporary capability.

Chromium. The  $(n;n',p)$  reaction thresholds of the chromium isotopes exceed 10 MeV with the single exception of Cr-50 where the threshold is very near 10 MeV and the isotopic abundance is low. Thus the  $(n;n',p)$  process in chromium seems to be of no FBR interest.

Cobalt (32). The  $(n;n',p)$  threshold is relatively low, the element is monoisotopic and the  $(n;n',p)$  cross section may be relatively large even at 10 MeV. There appear to be no quantitative measurements of the process below 10 MeV and the reaction product is stable. However, the cross section of the companion  $(n;p)$  reaction has an unusual energy dependence that could be attributed to a strong competition from a large  $(n;n',p)$  process. Whatever the above uncertainties they appear of little FBR concern as cobalt is a very minor FBR component and its  $(n;n',p)$  reaction of no dosimetry use.

Vanadium (19). The threshold for the  $(n;n',p)$  reaction is above 8 MeV. The reaction product is stable and thus activation techniques are of no use. Present experimental information must be construed from hydrogen-production measurements at  $\sim 15$  MeV (38). Theoretical extrapolation indicates that the cross section is  $\sim 5$  mb at 10 MeV and falling rapidly with energy. Thus the reaction appears to be of no FBR interest.

Titanium (17). All  $(n;n',p)$  reaction thresholds of the titanium isotopes exceed 10 MeV and thus these reactions are not relevant to the scope of the present remarks. They are noted here only because of the unusual sequential isotopic arrangement which makes it possible to determine detailed excitation functions for a number of the isotopes using reliable activation techniques. As a consequence these reactions can be useful "benchmarks" for theoretical-experimental comparisons.

### VIII. $(n;n',\alpha)$ CROSS SECTIONS

None of the  $(n;n',\alpha)$  thresholds are very low, all processes are inhibited by the barrier and the reaction products are generally stable.

*$(n;n',\alpha)$  processes do not make a major contribution to helium production in FBR systems and are thus of very minor interest.*

The cross sections below 10 MeV are not explicitly measured but rather inferred by theoretical extrapolation as outlined in Sec. X and elsewhere in these proceedings. The theory is generally founded upon measured helium-production cross sections and/or spectra determined in the favorable 14-15 MeV energy (38) or obtained by mass-spectrometric analysis of FBR-radiated samples (39). At 10 MeV the estimated  $(n;n',\alpha)$  cross sections are typically X 5-10 times smaller than the corresponding  $(n;\alpha)$  cross sections and the disparity increases as the nearby  $(n;n',\alpha)$  thresholds are approached.

The above general characteristics are illustrated by the following specific examples.

Iron. Several  $(n;n',\alpha)$  channels are energetically open below 10 MeV (see Table 1) but severely limited by the barrier. The resulting products are stable. At 10 MeV the elemental  $(n;n',\alpha)$  cross section is probably very small (ENDF-IV gives zero).

Nickel (14). The effective  $(n;n',\alpha)$  threshold is above 6 MeV and the reaction products stable. The theoretically estimated 10 MeV cross section is uncertain by 50-100% but X 5-10 smaller than the  $(n;\alpha)$  cross section and it decreases rapidly as the threshold is approached.

Chromium. All prominent  $(n;n',\alpha)$  reaction products are stable and the process should be similar to that of nickel with the primary contribution to helium production from the  $(n;\alpha)$  process. These assumptions can not be verified as CINDA 76/77 sites no relevant experimental information. It should be noted that the thresholds are higher for Cr than for Ni.

Cobalt (32). The reaction products are stable and there is no direct experimental knowledge of the  $(n;n',\alpha)$  cross section. The threshold is high and the cross section should be small at  $\sim 10$  MeV. Furthermore, there is no evidence in the well known  $(n;\alpha)$  for strong competition from the  $(n;n',\alpha)$  channel.

Vanadium (19). The  $(n;n',\alpha)$  threshold is high ( $>10$  MeV) and even at 14-15 MeV experimental evidence indicates a small ( $\sim 10$  mb) cross section.

Titanium (17). The  $(n;n',\alpha)$  thresholds are  $>8$  MeV for all the isotopes and most reaction products are stable. Neither  $(n;\alpha)$  nor  $(n;n',\alpha)$  cross sections are well known but theoretical extrapolation from helium-production values obtained at 14-15 MeV indicates that the  $(n;n',\alpha)$  reaction makes a relatively small contribution to helium-production at energies of  $\sim 10$  MeV.

The  $(n;n',\alpha)$  process is also energetically possible in the  $A \sim 100$  region but more severely inhibited by the barrier than in the  $A \sim 50$  region. The cross sections are generally very small at energies of  $\sim 10$  MeV and not relevant to FBR systems.

#### IX. $(n;2n')$ CROSS SECTIONS

FBR interest in the  $(n;2n)$  reaction is primarily confined to the region  $A \sim 50$ . Here, these cross sections are characterized by relatively high thresholds generally exceeding 10 MeV. The few exceptions are largely confined to the odd isotopes of low abundance. The only possible  $(n;2n')$  reaction in iron at  $E_n < 10$  MeV is that of Fe-57 (2.2% abundant) with a threshold of 7.78 MeV. Possible  $(n;2n')$  reactions in nickel at  $E_n < 10$  MeV are due to Ni-61 and -64 with thresholds of 7.95 and 9.66 MeV, respectively. Both isotopes are of low ( $\sim 1\%$ ) abundance. The energetically possible  $(n;2n')$  processes in chromium at  $E_n < 10$  MeV are with the isotopes Cr-53 and -54. The minimum threshold is 8.25 MeV and both isotopes are of low abundance. The two odd isotopes of titanium (47 and 49) have  $(n;2n')$  thresholds between 8 and 10 MeV but the isotopic abundances are low and the cumulative cross section amounts to only  $\sim 6$  mb at 10 MeV. Neither cobalt, manganese or vanadium have  $(n;2n')$  thresholds of less than 10 MeV. In view of the above, there is very little fast reactor interest in  $(n;2n')$  cross sections near  $A \sim 50$ . What interest there is appears to be associated with very high-burnup dosimetry applications and generally above the 10 MeV upper limit of the present discussion (e.g., Ni-58( $n;2n'$ ) and Co-59( $n;2n'$ )).

A number of nuclides in the region  $A \sim 100$  have  $(n;2n')$  thresholds in the range 8-10 MeV and the cross sections can amount to several tenths of a barn at 10 MeV. This behavior is illustrated by Nb-93 where the cross section rises rapidly from the threshold at 8.9 MeV to  $\sim 0.3$  b at 10 MeV (21). These  $(n;2n')$  cross sections in the region  $A \sim 100$  can be of considerable interest in some applications (e.g., fusion systems) but are not generally relevant to FBR systems.

It is concluded that:

*(n;2n')* processes in FBR structure materials are of minor importance due to high thresholds and low isotopic abundances. Therefore, results obtained via theoretical extrapolation from available data will probably suffice.

## X. THEORETICAL APPLICATIONS

In concert with the above experimental discussion it is appropriate to cite examples of the application of theory to the extrapolation and interpretation of measured quantities. More explicit theoretical discussion is given elsewhere in these proceedings.

In the few-MeV region the neutron interaction with primary FBR structural materials is a complex, fluctuating and only partially understood interplay of compound- and direct-reaction processes.

*Theory alone can not provide for FBR needs to 5-10% accuracies. It can be a useful tool for extrapolating measured quantities, estimating those that are unmeasured and for testing the physical validity of evaluated data sets.*

Energy-averaged models are conventionally based upon optical- and statistical-model concepts with the starting point being the calculation of the total cross section; one of the few unambiguously calculable quantities. At this very beginning there is already trouble as the experimental data can be very uncertain (see Sec. II) with consequent impact on the model. The frequent inability of global high-energy-based models to describe the neutron total cross section in the 0.5-2. MeV range and the frequently observed differences between models based upon low- and high-energy experiments may, in part, be due to the dubious nature of the experimental foundation. It is noted that improved energy-averaged total cross sections tend to resolve these discrepancies.

*A first criteria for an energy-averaged model is consistency with the measured total cross section over a wide energy range.*

The capability of measurements to provide accurate neutron total cross sections is a near unique attribute of model interpretations based upon neutron interactions. This potential has not been fully exploited.

Spherical optical-model fits to isolated elastic scattering distributions in the region  $A \sim 50$  are a legion. They can be very descriptive as illustrated in Fig. 37 (19). At higher energies they are in default as they ignore the known vibrational character of the nuclides. In the low-MeV region they are little more than costly parameterizations of local fluctuations with little reality in a broader scope.

*Energy-averaged interpretations of elastic distributions have meaning only in the context of broad averages transcending local and intermediate structure fluctuations.*

It is difficult to obtain a proper average below 5 MeV due to the restrictions of the experimental resolution and the uncertainties in the character of the

contributing reaction channels. Even with a proper average there remain the physical uncertainties of fluctuation corrections, channel correlations and the admixture of direct and compound-nucleus processes (5). The effect of these physical uncertainties can be large as illustrated by the titanium example of Figs. 38 (5). In this case, the model, based upon a broad (1 MeV) average of measured results, can not describe the explicit distributions in detail. However, beyond these fluctuation effects are the uncertainties in the correction factors that can be as large in both the elastic and inelastic channels. There is the additional matter of vibrational coupling of ground- and excited-state transitions which, in the case of titanium, are a matter of continuing study that may now have cost more than the original measurements.

*Models in the  $A \sim 50$ , few-MeV region are of marginal use in directly providing quantitative elastic scattering data for FBR use.*

In some cases, such as chromium, the experimental results are deficient and there is little alternative to a qualitative model interpretation.

At higher energies compound-nucleus processes are a minor factor and the elastic scattering is very largely a "shape" process. In this region the models can be very useful in extrapolating the measured angular range particularly if the total cross section is made a stringent constraint. Unfortunately, this evaluation procedure has not been very widely used.

The same experimental and physical problems inhibiting the quantitative calculation of elastic scattering in the region of  $A \sim 50$  effect the calculation of inelastic processes. The example of titanium, shown in Figs. 14 and 39, is illustrative of the prominent fluctuations in the inelastic channels and of the problems of correcting the common Hauser-Feshbach statistical formula. The experimental values generally lie between the two extremes defined by entirely isolated and fully overlapping resonances. The range between these two limits is 25-50%, well beyond the accuracies often sought by the FBR programs. Calculations can be useful in extrapolating inelastic cross sections to threshold and can give guidance in the interpretation of experiments involving a strong angular dependence of the emitted neutrons. They do not independently provide inelastic cross sections to 5-10% accuracies. Moreover, the range of calculational capability is further restricted by the limited knowledge of the characteristics of the contributing channels.

Thus, generally in the region  $A \sim 50$ ;

*Theory is a secondary and not a primary source of FBR total and scattering cross sections.*

It is best employed as an extrapolational tool when tailored to the particular problem at hand.

The above problems are alleviated in the  $A \sim 100$  region and FBR needs for total and scattering cross sections are more modest. Thus theoretical extrapolation is more useful than in the  $A \sim 50$  region. Calculated results are quantitatively consistent with measured total and elastic-scattering cross sections over wide energy-angle ranges as illustrated by the molybdenum and zirconium results of Figs. 12 and 13 (22,23). Comparisons such as these give confidence to

calculational extrapolations in this region to accuracies of  $\sim 10\%$  including the provision of unmeasurable fission-product cross sections. Thus:

*Many FBR needs for total and elastic-scattering cross sections in the  $A \sim 100$  region can be met by calculational extrapolation from the available data.*

At energies above  $\sim 5$  MeV several global models are capable of providing for most total and elastic-scattering cross section needs in this region (42). The inelastic-scattering calculational capability in the  $A \sim 100$  region is more limited as illustrated by the Zr-92 and Mo-100 example of Figs. 23 and 24 (22). Spins and parities are not generally known at excitations of more than several MeV, the interaction is frequently a complex mixture of direct and compound-nucleus reactions and fluctuation corrections remain a troublesome matter. Even with these obstacles, calculational extrapolation can materially contribute to the provision of inelastic scattering data in this mass region particularly in view of the relatively modest FBR requirements. It should be noted that calculational capability in the  $A \sim 100$  region is not demanding of model refinements, such as iso-spin and parity dependence, though these aspects are of basic physical interest.

It has been suggested (43) that theory based upon energy-averaged results and verified against a few very-high-resolution total cross section measurements has the potential for statistically defining the fluctuating structure in the MeV range in all contributing channels in a physically licit manner. In a sense, it is an extrapolation from the available experimental data into a region that will remain very difficult to measure with very good resolution. The concept has the practical attractiveness of inherently providing resonance descriptions that are manageable from a reactor-calculation point of view. Thus far the approach has been attempted in only a limited and qualitative manner (44).

The essential importance of theoretical extrapolation in the provision of reaction cross sections has been emphasized in the above experimental sections. Such extrapolations generally take two forms. First, an extrapolation in energy from measured values toward threshold. This is a sound mechanism for the provision of dosimetry data in the important and difficult-to-measure region very near threshold. It is also an effective way of extending important measured cross sections into the region of primary FBR interest (e.g.,  $(n;p)$  and  $(n,\alpha)$  cross sections below 10 MeV). Secondly, an extrapolation in both reaction type and energy. Some important FBR reaction data is at present experimentally unknown and must be provided by calculations based either on global models or more limited extrapolation between neighboring reaction types. Many reactions leading to gas production in FBR systems are of this nature. The following paragraphs illustrate both types of calculational capability. Discussion of the underlying theories is to be found elsewhere (45).

The calculational tools are generally few- or multi-step Hauser-Feshbach procedures often with the addition of pre-equilibrium contributions. They generally make use of global potential parameters and generalized level-density distributions (46,47). Potentials specifically tailored to the particular

nuclide have seldom been employed. These formalisms are often of very broad scope and can be efficient in computer utilization. In the FBR region ( $<10$  MeV) the pre-equilibrium process is usually a minor consideration and the number of open channels is limited thus simplifying the computations. The present illustrations are taken from GNASH calculations of Young and Arthur (48) and from the somewhat simpler HAUSER calculations of Mann and Schenter (49). The  $(n;p)$  cross sections are frequently well known and can provide a benchmark for the calculational methods. Results calculated with GNASH are compared with a number of relatively well known  $(n;p)$  cross sections in Fig. 40. The calculated results are independent of the measured values and not fits to the data. Even so the relative energy-dependence of the calculated cross sections agrees with the measurements to within 10-40%.

*Calculations can quantitatively extrapolate detailed reaction measurements into the very low threshold region*

with accuracies that are useful in dosimetry applications. The extrapolations are not very sensitive to the details of the particular model. The same GNASH calculations applied to Ti-46 in a broader scope are illustrated in Fig. 41. Here the  $(n;p)$  cross section is experimentally well known but there is essentially no experimental knowledge of the  $(n;\alpha)$ ,  $(n;n',p)$  and  $(n;n',\alpha)$  cross sections. The model results are qualitatively consistent with the measured  $(n;p)$  cross sections to energies well above those of FBR interest. Thus there can be reasonable confidence in the calculated  $(n;\alpha)$ ,  $(n;n',p)$  and  $(n;n',\alpha)$  cross sections. The rapid rise of the  $(n;n',p)$  reaction and consequent competition with the  $(n;p)$  channel is often characteristic of these reactions in this region though these calculations seem to accentuate the effect. A similar example in vanadium is illustrated in Fig. 31. HAUSER calculations have been widely used to extrapolate fragmentary experimental information into the region of FBR interest particularly providing  $(n;\alpha)$  cross sections. The calculational methods giving reasonable qualitative agreement with  $(n;\alpha)$  cross sections in cobalt and  $(n;p)$  reactions in Fe-56 provide the unmeasured  $(n;\alpha)$  cross sections of Fe-56 as illustrated in Figs. 42, 43, and 44. Similar calculations were employed to extrapolate the vanadium  $(n,\alpha)$  cross section as shown in Fig. 36. Again, as outlined above in Sec. VI, a competition between  $(n;\alpha)$  and  $(n;n',\alpha)$  channels is evident. At present:

*Calculational extrapolation is the primary source of gas production data for FBR use.*

The overall accuracies are  $\sim 20-40\%$  and do meet many needs.

*A very few quantitative measurements of carefully selected cross sections at energies of less than 10 MeV would greatly enhance the capabilities of the calculations.*

This is particularly so in the areas of  $(n;\alpha)$ ,  $(n;n',p)$  and  $(n;n',\alpha)$  reactions.

The above models are particularly effective in the estimating of complex cross sections and emission spectra at energies above 10 MeV primarily of interest in other contexts (e.g., fusion systems) (45). An example is the multiple neutron emission processes in niobium shown in Fig. 45. Here the GNASH results are quantitatively description of  $(n;2n')$ ,  $(n;3n')$  and  $(n;2n')$ -isomer processes

to well above 20 MeV. At these higher energies many additional channels are open with rapid increases in experimental uncertainties and greater reliance on theoretical estimates.

Finally, a note of caution: Few, if any, complex model codes are "correct" in a wide scope. The "errors" range from inappropriate numerical methods to simple mistakes and incomplete or incorrect documentation and are in addition to the more basic problem of physical applicability. This unfortunate situation is enhanced by a lack of the general availability requisite for critical assessment of performance.

## XI. SYSTEM SENSITIVITIES

The above FBR structure data is more meaningful when viewed in the context of core performance. Therefore the impact of present and near-future structure-data uncertainties on important core parameters was assessed. The chosen parameters were: eigenvalue (i.e.,  $k_{eff}$ ), breeding ratio, central reaction rate ratios of  $^{238}\text{U}$  capture and fission relative to  $^{239}\text{Pu}$  fission, and the central reactivity worth of  $^{239}\text{Pu}$  and sodium. Nuclear data sensitivity coefficients (50) calculated for ZPR-9 Assembly 31, the Advanced Fuels Program benchmark critical assembly (51), were utilized to assess the impact of the structure-data uncertainties upon a representative contemporary-to-advanced FBR mixed-(Pu,U) carbide system. The data uncertainties were confined to the total and scattering cross sections of iron, nickel and chromium over the energy range 0.5-10 MeV, i.e., the scope of the present paper. Multigroup cross sections were produced by MC<sup>2</sup>-II (8) using ENDF/B Version IV nuclear data. Generalized sensitivity coefficients were obtained over 12 broad energy groups using the VARI-1D code (52). It was assumed that the uncertainties were uncorrelated. The impact of the data uncertainties upon the core parameters was then evaluated: 1) individually by element-reaction type, 2) collectively within a reaction type, and 3) as a whole. Of course, these comparisons do not address peripheral issues (such as shielding) and there are atypical core concepts where the impact of structure-data uncertainties may be much greater (e.g., SAREF). However, within the context of contemporary FBR core concepts, the calculated sensitivity to data uncertainties should be reasonably valid.

The estimates of the uncertainties in the total cross section and the elastic and inelastic scattering cross sections of Fe, Ni, and Cr has been discussed in the above data sections. The present and projected near-future uncertainties in these data are summarized in Fig. 46. These uncertainties have been combined with the sensitivity data to assess the impact upon calculated integral parameters. The sensitivity coefficients express the percent change in a reactor parameter per percent change in a particular cross section over a given energy range. In this manner, the effects of uncertainties in structure elastic and inelastic scattering cross sections on FBR integral parameters were obtained. These results are summarized in Tables 2 and 3. Before analyzing these results, the following points should be considered. The effects of a cross section change (or uncertainty) will differ at different energies not only in magnitude, but perhaps also in sign. That is, the effect on an integral parameter of a cross section change over a large energy range, as considered here (0.5-10 MeV), may include some cancellation of positive and

negative effects. Secondly, the effects of uncertainties in the cross sections of each of the materials Fe, Ni, and Cr were combined as though the errors were completely uncorrelated. Combining the effects of both elastic and inelastic scattering uncertainties as though these data were uncorrelated is one possible, though not especially realistic, hypothesis. Clearly, since the total cross sections are better known, these provide an additional constraint upon the sum of the elastic and non-elastic cross sections. This is important since the impacts of particular changes in the elastic and inelastic scattering cross sections often have opposite effects. However, since an increase in elastic scattering might justify a decrease in the inelastic scattering cross section, these are likely to produce a similar or additive effect (i.e., greater than simply the addition in quadrature based on no correlation between the uncertainties).

Consider now the results in Tables 2 and 3. The present uncertainties in the elastic scattering cross section for each of these isotopes produce less than 0.1% uncertainty in eigenvalue, breeding ratio, and central reaction rate ratios, and less than 0.5% in central reactivity worths. The effects of present uncertainties in the inelastic scattering cross sections for these isotopes are only slightly greater. The uncertainty in  $k_{eff}$  is  $\sim 0.1\%$  for both the Fe and Ni inelastic scattering data uncertainties. The uncertainty in the spectral index  $f^{28}/f^{49}$  is  $\sim 1.5\%$ , due principally to the uncertainty in the Fe inelastic scattering cross section. This small spectral impact also changes the sodium worth by  $\sim 1\%$ . For both the elastic and inelastic scattering cross sections, these effects are reduced by about a factor of 2 with the projected near-future uncertainties. The combined effects of both the elastic and inelastic scattering data uncertainties for all three isotopes may be estimated by adding in quadrature the results in both Tables 2 and 3. The total effects of present uncertainties are: 0.16% in eigenvalue, 0.07% in breeding ratio, 0.15% in  $c^{28}/f^{49}$ , 1.44% in  $f^{28}/f^{49}$ , and 0.31% and 1.15% in the central worth of  $^{239}\text{Pu}$  and sodium; the effects of total projected uncertainties are: 0.08% in eigenvalue, 0.04% in breeding ratio, 0.08% in  $c^{28}/f^{49}$ , 0.67% in  $f^{28}/f^{49}$ , and 0.57% in the central worth of  $^{239}\text{Pu}$  and sodium.

In order to put the above uncertainties in perspective, one must consider the uncertainties in the measurement of these integral parameters. The uncertainty in criticality or  $k_{eff}$  is  $\sim 0.5\%$  and in relative reaction rates and material reactivities it is  $\sim 2-5\%$ . Thus, the uncertainties in calculated integral parameters resulting from the uncertainties in the structure scattering data above 0.5 MeV are relative small. The sensitivities in the lower energy range (i.e., below 0.5 MeV) are comparable in magnitude for the elastic scattering cross sections (and, of course, zero for the inelastic scattering cross sections) from these materials. The effects are also small in a relative sense. That is, there is relatively little to gain (in reducing uncertainties in calculated FBR core integral parameters) through improving the total and scattering cross sections of the structural materials as compared to the impact of data uncertainties in the principal cross sections of  $^{239}\text{Pu}$  and  $^{238}\text{U}$ .

The above FBR system sensitivity results can be summarized as follows:

*The uncertainties in calculated integral parameters produced by uncertainties in the structure-scattering data above 0.5 MeV are significant, but small relative to the effects of other nuclear data uncertainties.*

*The present uncertainties in the structure-elastic-scattering cross sections produce  $\sim 0.1\%$  uncertainty in  $k_{eff}$ .*

*The present uncertainties in the structure-inelastic-scattering cross sections produce  $\sim 0.1\%$  uncertainty in  $k_{eff}$ .*

*The projected near-future uncertainties in these structure-scattering data will decrease the effects upon calculated FBR integral parameters by about a factor of two.*

## XII. GENERAL COMMENTS

Associated with the above specific technical remarks are some general comments.

There is an outstanding need for renewed attention to standard-reference properties. This is particularly true of secondary standards useful in particular types of measurements. There are not generally accepted sets of such secondary standards for use in ratio measurements and subsequent renormalization is difficult or even impossible. In some areas (e.g. (n;p) cross sections) there frequently is no merit in further measurements until the standard uncertainties are resolved as they are dominant factors. Less basic but important is the use of redundant verification standards in any measurement with a high-accuracy objective. The standard issues extend from the common matters of flux and cross-section to decay properties, half-lives, emission spectra, etc. In the latter diverse areas a double or even triple tier of standard-references is frequently encountered. Thus an outstanding issue remains:

*The identification, recognition, acceptance and provision of flux, cross-section and associated reference standards.*

In so far as possible, all data should be reported in a manner permitting subsequent renormalization to the best contemporary standards. It is doubtful if many of the precision FBR cross section needs will be provided for until these standard issues are resolved.

Accuracy appears to be a two dimensional quantity - one axis stretching from the microscopic to the integral and the other geographic. Some integral measurements (e.g., fission ratios, responses in integral fields, etc.) are reported to accuracies of 1% or better. This is an awesome precision not realized in similar microscopic measurements even in much simpler environments. Yet the discrepancies are often attributed to shortcomings in microscopic data. It also seems that the western hemisphere may be more conservative in the judgement of microscopic data uncertainties. Further, there may be some general inverse relationship between stated precision and the experience of the research group. Microscopic-cross-section accuracies of 1-3% are exceedingly difficult to realize even in the simple cases of self normalizing and broad resolution transmission measurements. A realistic contemporary guideline for the best microscopic-partial-cross-section measurement appears to be 5%

in the more easily studied cases and measured results from different sources seldom are consistent to this accuracy. It is encouraging to note that FBR microscopic accuracy requirements do not generally exceed measurement capability.

Conventional activation techniques have a surprisingly wide applicability to data problems. Where suitable they should be fully exploited as they have generally provided the more precise results.

New and novel techniques should be sought beyond matters of scale such as increased source intensity and longer flight path. The objective is new concepts with the potential for very large impact such as is illustrated by that of the advent of the GeLi detector on the entire dosimetry field. Low-energy photon detection may have such a potential in certain applications.

Precise data is demanding of detailed correction procedures. The computational tools for such corrections are generally available but not sufficiently used. In some instances uncertainties due to correction procedures have exceeded those in the actual measurements themselves. Moreover, the computational capability is now such as to permit a detailed simulation and optimization of the experiment prior to measurement. This capability is seldom, if ever, exploited.

There tends to be a void between consumer and producer that can not really be filled by the middle-man function of the evaluator. A closer relationship between producer and consumer is long overdue with a much better correlation of integral-experiment and calculation with data measurement-evaluation. Moreover, the latter should be a unified experimental-theoretical-evaluation endeavor. Integral testing should be a joint activity of both producer and consumer particularly as carried out in the simplest and most understandable of environments. Such tests are essential: to the validation of the microscopic data, to the verification of calculational methods, and for providing guidance of the overall data programs in a scope far transcending the FBR needs.

Finally, the above technical remarks are stringently focused on FBR needs. The view is myopic and a broad data base suitable for a diversity of nuclear-energy applications is the bigger objective. The unfortunate consequences of undue emphasis on a particular concept (e.g. U/Pu FBR cycles) have recently been demonstrated. The data base should be of a broad scope that will be responsive to the needs of a variety of energy concepts that will change as the consequence of technological advances. Engineering expediency in a limited context should not be allowed to distort the physical data base in such a manner as to prejudice its application in a future and wider scope.

#### ACKNOWLEDGEMENTS

The authors are indebted to Drs. P. Young, E. Arthur and F. Mann for making available results of model calculations and to the National Nuclear Data Center (Brookhaven National Laboratory) for providing extensive numerical and graphical data.

## REFERENCES\*

1. Herein, FBR relevance is defined as stated in WRENDA-76/77.
2. A. Smith and J. Whalen, Argonne Natl. Lab. Report, ANL/NDM-33 (1977).
3. J. Harvey et al., Priv. Com. (1977).
4. A. Smith, Priv. Com. (1977).
5. P. Guenther et al., Argonne Natl. Lab. Report ANL/NDM-31 (1977).
6. R. Schwartz et al., Natl. Bur. Stds. Pub., NBS-138 (1974).
7. P. Stoler et al., CONF-710301 (I), P-311 (1971).
8. H. Henryson et al., Argonne Natl. Lab. Report, ANL-8144 (1976).
9. See for example, Computing Methods in Reactor Physics, H. Greenspau et al., Gordon and Breach, NY (1968).
10. D. Smith, Nucl. Sci. and Eng., 64 897 (1977).
11. D. Reitmann and A. Smith, Priv. Com. (1977).
12. B. Holmquist and T. Wiedling, Atomenergi Sweden Report, AE-403 (1971).
13. W. Kinney and F. Perey, Oak Ridge Natl. Lab. Report, ORNL-4515 (1970).
14. P. Guenther et al., Argonne Natl. Lab. Report, ANL/NDM-11 (1975).
15. F. Perey et al., Oak Ridge Natl. Lab. Report, ORNL-4523 (1970).
16. W. Kinney and F. Perey, Oak Ridge Natl. Lab. Report, ORNL-4806 (1974).
17. C. Philis et al., Argonne Natl. Lab. Report, ANL/NDM-28 (1977).
18. W. Kinney and F. Perey, Oak Ridge Natl. Lab. Report, ORNL-4810 (1973).
19. P. Guenther et al., Argonne Natl. Lab. Report, ANL/NDM-24 (1977).
20. F. Perey and W. Kinney, Oak Ridge Natl. Lab. Report, ORNL-4551 (1970).
21. A. Smith et al., Zeits Phys., 264 379 (1973).
22. A. Smith et al., Nucl. Phys., A244 213 (1975).
23. P. Guenther et al., Phys. Rev., C12 1297 (1975); see also Argonne Natl. Lab. Report, ANL/NDM-4 (1974).
24. D. Smith, Argonne Natl. Lab. Report, ANL/NDM-20 (1976).
25. D. Reitmann et al., Natl. Bur. Stds. Pub., NBS-425 (1975).
26. W. Kinney and F. Perey, Nucl. Sci. and Eng., 63 418 (1977).
27. D. Smith and J. Meadows, Argonne Natl. Lab. Report, ANL/NDM-10 (1975).
28. D. Smith, Argonne Natl. Lab. Report, ANL/NDM-30 (1977). See also Ref. 29.
29. D. Smith, Argonne Natl. Lab. Report, ANL/NDM-34 (1977).
30. M. Bhat, Priv. Com. (1977).
31. J. Roy and J. Hawton, Chalk River Report, CRC-1003 (1960).

\*A number of secondary references are cited in the primary references.

32. P. Guenther et al., Argonne Natl. Lab. Report, ANL/NDM-1 (1973).
33. D. Smith and J. Meadows, Nucl. Sci. and Eng., 60 187 (1977).
34. A. Calmand, IAEA Tech. Report No. 156 (1974).
35. L. Greenwood and R. Heinrich, Brookhaven Natl. Lab. Report, BNL-NCS-50681 (1977).
36. C. Philis et al., Argonne Natl. Lab. Report, ANL/NDM-27 (1977).
37. M. Vlasov et al., Proc., Inter. Conf. on Interaction of Neutrons with Nuclei, CONF-760715 (1976).
38. R. Haight et al., elsewhere in these proceedings.
39. H. Farrar et al., Priv. Com. (1977).
40. A. Paulsen et al., Atomkern Energie, 22 291 (1974).
41. A. Smith et al., Argonne Natl. Lab. Report, ANL/NDM-6 (1975); see also J. Frehaut, Proc. Inter. Conf. on Interaction of Neutrons with Nuclei, CONF-760715 (1976).
42. J. Rapaport et al., Proc. Symposium on Neutron Cross Sections from 10-40 MeV, BNL-NCS-50681, p. 257 (1977).
43. P. Moldauer, Priv. Com. (1977).
44. E. Barnard et al., Argonne Natl. Lab. Report, ANL/NDM-3 (1973).
45. See, for example, Proc. Symposium on Neutron Cross Sections from 10-40 MeV, BNL-NCS-50681 (1977).
46. See, for example, F. Berchetti and G. Greenlees, Phys. Rev., 182 1190 (1969); D. Wilmore and P. Hodgson, Nucl. Phys., 55 673 (1964); and F. Perey, Phys. Rev., 131 745 (1963).
47. A. Gilbert and A. Cameron, Can. Jour. Phys., 43 1446 (1965).
48. E. Arthur and P. Young, Brookhaven Natl. Lab. Report, BNL-NCS-50681 (1977).
49. F. Mann and R. Schenter, Brookhaven Natl. Lab. Report, BNL-NCS-50681 (1977).
50. R. McKnight, Trans. Am. Nucl. Soc., 27 (1977).
51. R. Pond et al., Argonne Natl. Lab. Report, to be published.
52. W. Stacey and J. Regis, Argonne Natl. Lab. Report, to be published.

TABLE 1. Reaction Q-values\*

| Isotope | % Abundance | Q-values (MeV) |                |          |                   |
|---------|-------------|----------------|----------------|----------|-------------------|
|         |             | (n;p)          | (n; $\alpha$ ) | (n;n',p) | (n;n', $\alpha$ ) |
| Fe-54   | 5.8         | 0.087          | 0.84           | -8.854   | -8.42             |
| Fe-56   | 91.7        | -2.918         | 0.32           | -        | -7.62             |
| Fe-57   | 2.2         | -1.780         | 2.40           | -        | -7.33             |
| Ni-58   | 67.9        | 0.394          | 2.89           | -8.177   | -6.41             |
| Ni-60   | 26.2        | -2.041         | 1.35           | -9.532   | -6.30             |
| Cr-50   | 4.3         | -0.256         | 0.32           | -9.588   | -8.56             |
| Cr-52   | 83.8        | -3.195         | -1.21          | -        | -9.35             |
| Cr-53   | 9.6         | -2.640         | 1.79           | -        | -9.15             |
| Co-59   | 100.0       | -0.783         | 0.32           | -7.369   | -6.95             |
| V-51    | 99.8        | 0.719          | -2.05          | -8.052   | -10.29            |
| Ti-46   | 7.9         | -1.584         | -0.08          | -        | -8.01             |
| Ti-47   | 7.3         | 0.182          | 2.18           | -        | -8.96             |
| Ti-48   | 73.9        | -3.208         | -2.03          | -        | -9.45             |
| Ti-49   | 5.5         | -              | 0.28           | -        | -10.17            |
| Ti-50   | 5.3         | -              | -3.44          | -        | -10.72            |

<sup>a</sup>Reactions limited to relatively abundant isotopes and to thresholds  $\lesssim 10$  MeV.

TABLE 2. Effects of Uncertainties in Structure Elastic Cross Sections on FBR Integral Parameters\*

| Percent Change in:           | Considering Present Uncertainties<br>in $\sigma_{el}$ of |        |        |       | Considering Projected Uncertainties<br>in $\sigma_{el}$ of |        |        |       |
|------------------------------|--|--------|--------|-------|--|--------|--------|-------|
|                              | Fe   | Ni     | Cr     | RMS** | Fe   | Ni     | Cr     | RMS** |
| Eigenvalue, $k_{eff}$        | .0763  | .0116  | .0438  | .0887 | .0442  | .0066  | .0145  | .0470 |
| Breeding Ratio               | -.0548   | -.0071 | -.0334 | .0646 | -.0302   | -.0039 | -.0088 | .0317 |
| Central Reaction Rate Ratios |  |        |        |       |  |        |        |       |
| $c^{28}/f^{49}$              | .0157  | .0028  | .0068  | .0174 | .0100  | .0017  | .0032  | .0106 |
| $f^{28}/f^{49}$              | -.0548   | -.0126 | -.0735 | .0925 | -.0363   | -.0080 | -.0194 | .0420 |
| Central Material Worths      |  |        |        |       |  |        |        |       |
| $^{239}\text{Pu}$            | .1616  | .0231  | .0962  | .1895 | .0922  | .0132  | .0289  | .0975 |
| $^{23}\text{Na}$             | .4781  | .0652  | .2167  | .5290 | .2683  | .0365  | .0783  | .2819 |

\* All changes in the above reactor integral parameters are given in percent. The sign is included in the components to indicate the direction the parameter changes when the elastic scattering cross section is increased.

\*\*Represents the root-mean-squared combination of the effects of uncertainties in Fe, Ni, and Cr.

TABLE 3. Effects of Uncertainties in Structure Inelastic Cross Sections on FBR Integral Parameters\*

| Percent Change in:           | Considering Present Uncertainties<br>in $\sigma_{inel}$ of |        |        |        | Considering Projected Uncertainties<br>in $\sigma_{inel}$ of |        |        |       |
|------------------------------|--|--------|--------|--------|--|--------|--------|-------|
|                              | Fe   | Ni     | Cr     | RMS**  | Fe   | Ni     | Cr     | RMS** |
| Eigenvalue, $k_{eff}$        | -.0936   | -.0248 | -.0901 | .1323  | -.0584   | -.0113 | -.0260 | .0649 |
| Breeding Ratio               | .0281  | .0042  | .0159  | .0325  | .0168  | .0020  | .0039  | .0174 |
| Central Reaction Rate Ratios |  |        |        |        |  |        |        |       |
| $c^{28}/f^{49}$              | .1308  | .0187  | .0686  | .1489  | .0720  | .0086  | .0184  | .0748 |
| $f^{28}/f^{49}$              | -1.2978  | -.1596 | -.5934 | 1.4359 | -.6621   | -.0728 | -.1693 | .6873 |
| Central Material Worths      |  |        |        |        |  |        |        |       |
| $^{239}\text{Pu}$            | .2245  | .0274  | .1019  | .2481  | .1149  | .0125  | .0293  | .1192 |
| $^{23}\text{Na}$             | -.9375   | -.1132 | -.3946 | 1.0235 | -.4747   | -.0511 | -.1181 | .4918 |

\*All changes in the above reactor integral parameters are given in percent. The sign is included in the components to indicate the direction the parameter changes when the inelastic scattering cross section is increased.

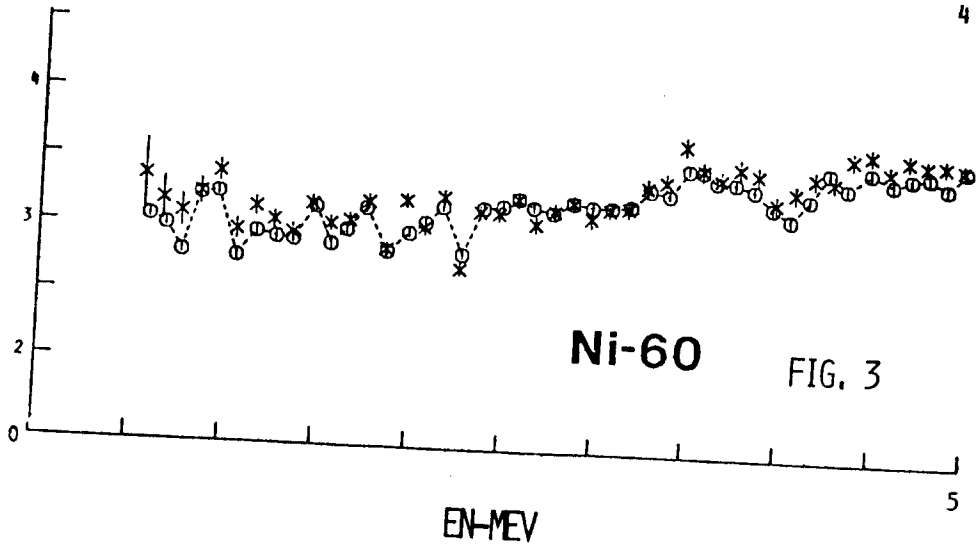
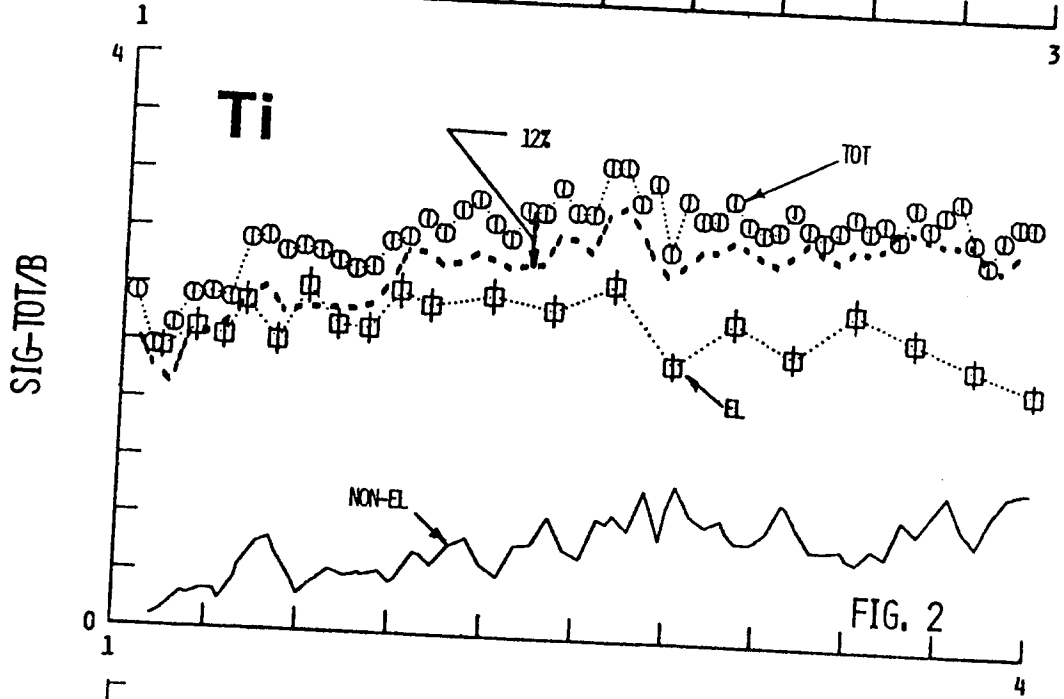
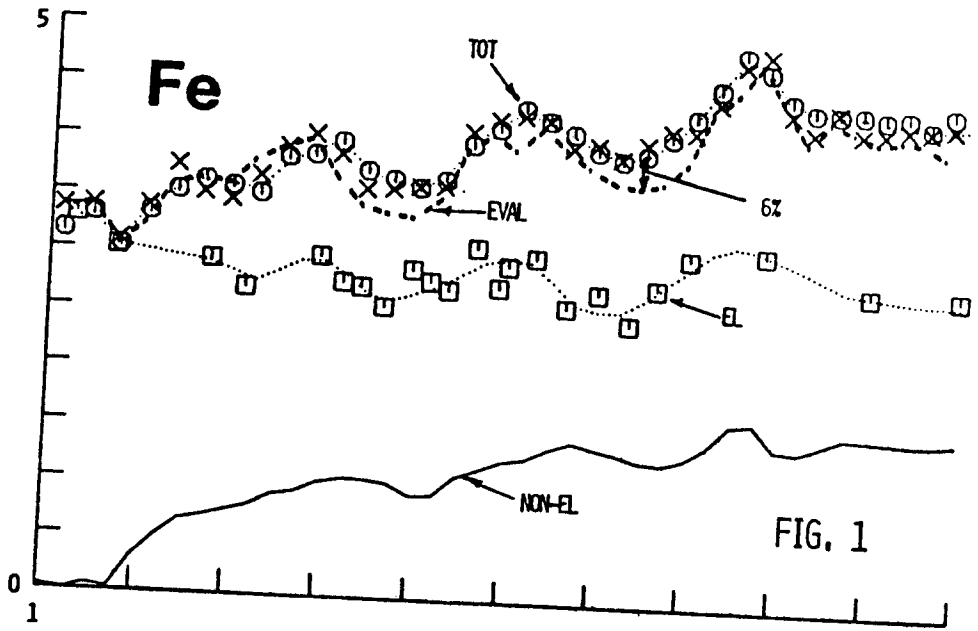
\*\*Represents the root-mean-squared combination of the effects of uncertainties in Fe, Ni, and Cr.

## FIGURE CAPTIONS

1. Comparison of Broad-resolution Iron Total Cross Sections (0, Ref. 2) with Equivalent Averages of: 1) ENDF-IV (dashed curve), and 2) High resolution Results of Harvey et al. (3) (X). Angle-integrated elastic scattering cross sections are indicated by squares (4). Dotted and solid curves are eye-guides for total, elastic and inelastic cross sections.
2. Comparison of Measured Broad-resolution (0, Refs. 1 and 5) and Equivalent Average of Fine-resolution (---, Ref. 6) Titanium Total Cross Sections. Squares indicate angle-integrated elastic scattering cross sections (6). Dotted and solid curves are total and scattering cross-section eye-guides.
3. Comparison of Broad-resolution Total Cross Sections of Ni-60 (0, Ref. 4) with an Equivalent-average of High Resolution Results (x, Ref. 7).
4. Monte Carlo Simulation of a Broad-resolution (30 keV) Measurement of Elastic Scattering from Iron (1). Character of "observed" distributions is very dependent on mean incident energies.
5. Differential Elastic-scattering Cross Sections of Iron. Data for  $E_n \leq 4.0$  MeV from Ref. 4; for  $E_n > 4.0$  MeV from Refs. 12 and 13. Curves represent Legendre fits to data<sub>n</sub> points.
6. Differential Elastic-scattering Cross Sections of Natural Nickel. Data from Refs. 14 ( $E_n \leq 4$  MeV) and 15 ( $E_n > 4$  MeV). Curves represent fit to data.
7. Differential Elastic-scattering Cross Sections of Ni-60. Data from Ref. 4. Curves indicate fit to data.
8. Differential Elastic-scattering Cross Sections of Chromium. Data from Refs. 4 ( $E_n < 1.5$  MeV) and 12 + 16 ( $E_n > 2.0$  MeV). Curves indicate fit to data.
9. Differential Elastic scattering Cross Sections of Titanium. Data base and notation is similar to that of Fig. 5 (Refs. 5, 17 and 18).
10. Differential Elastic Scattering Cross Sections of Vanadium. Notation is similar to that of Fig. 4. Data from Refs. 19, 12 and 20.
11. Differential Elastic-scattering Cross Sections of Niobium. Notation is similar to that of Fig. 4. Data from Ref. 21.
12. Differential Elastic-scattering Cross Sections of the Even Isotopes of Molybdenum. Data from Ref. 22. Curves note model calculations.
13. Differential Elastic-scattering Cross Sections of Some Even Isotopes of Zirconium. Notation is similar to that of Fig. 12. Data from Ref. 23.

14. Comparison of High-resolution  $(n;n',\gamma)$  (26) and Medium-resolution  $(n;n')$  and  $(n;n',\gamma)$  Cross Sections (24) for the Excitation of the 847 keV State in Iron.
15. Comparison of Medium-resolution  $(n;n')$  and  $(n;n',\gamma)$  Cross Sections for the Excitation of the 847-keV State in Iron with an Equivalent Average Constructed from ENDF-IV (24).
16. Inelastic Neutron Excitation Cross Sections of Iron (4). Solid curves indicate eye-guide  $\pm$  noted uncertainty. Dotted curves indicate ENDF-IV.
17. Cumulative Inelastic-scattering Excitation Cross Sections of Iron (4) (solid curve) Compared with ENDF-IV (dotted curve).
18. Inelastic-excitation Cross Sections of Natural Nickel Taken from Refs. 14 and 15. Solid curves are eye-guides, dotted curves ENDF-IV.
19. Inelastic-excitation Cross Sections of Ni-60 (4 and 15). Curves are eye-guides.
20. Inelastic-excitation Cross Sections of Vanadium (14). Curves are proposed ENDF-V.
21. Inelastic-excitation Cross Sections of Elemental Titanium (5 and 17). Curves are proposed ENDF-V.
22. Inelastic-excitation Cross Sections of Niobium. Solid curves indicate ENDF-IV, dotted lines results of model calculations (21).
23. Inelastic-excitation Cross Sections of Mo-100. Results are representative of those for the other even isotopes (22). Measured results are noted by points; curves are the result of model calculation.
24. Inelastic-excitation Cross Section of Zr-92 (23). Results are also representative of Zr-90. Curves are the results of model calculations outlined in Ref. 23.
25. Fe-56  $(n;p)$  Cross Sections. Figure taken from Vlasov et al. (37).
26. Fission-spectrum Response of Fe-54 and Fe-56  $(n;p)$  Reactions.
27. Fe-54  $(n;p)$  Cross Sections.
28. Ni-58  $(n;p)$  Cross Sections. See Ref. 27 for definition of specific data values.
29. Ni-60  $(n;p)$  Cross Sections. Data referenced in 14. Curve is ENDF-IV.
30. Co-59  $(n;p)$  Cross Sections (32). Curve is ENDF-IV. Data referenced in BNL-325.
31. V-51  $(n;p)$  Cross Sections. Data referenced in 19. Dashed curve is ENDF-IV, solid curve evaluation of Ref. 19.

32. Ti-46 (n;p) Cross Sections. Data referenced in V-36. Dashed curve is ENDF-IV, solid curve evaluation of Ref. 36.
33. Ti-47 (n;p) Cross Sections. Notation same as for Fig. 32.
34. Ti-48 (n;p) Cross Sections. Notation same as for Fig. 32.
35. Co-59 (n; $\alpha$ ) Cross Sections. Figure taken from M. Vlasov et al. (37).
36. V-51 (n; $\alpha$ ) Cross Sections. Figure taken from Ref. 19. Solid curve indicates evaluation of Ref. 19 and dotted curve ENDF-IV. Squares indicate experimental results of Paulsen et al. (40).
37. Comparison of Measured (O) and Model Calculated (—) Elastic Scattering Cross Sections of Vanadium (19). Energies are noted in MeV.
38. Measured and Calculated Scattering Cross Sections of Titanium (5). Data is represented by (O), calculations by curves with H = Hauser-Feshbach and W = with fluctuation correction. Energies are given as incident/excitation in MeV.
39. Inelastic Scattering Cross Sections of Titanium. Figure is similar to Fig. 21 extended to include Hauser-Feshbach calculated results with (····) and without (---) fluctuations correction.
40. Comparison of Measured and Calculated (n;p) Cross Sections of Iron and Nickel. Calculations used computer code GNASH, courtesy of P. Young and E. Arthur.
41. Measured and Calculated (n;p) (n; $\alpha$ ) (n;n',p) and (n;n', $\alpha$ ) Cross Sections of Ti-46. Calculations by Arthur (48, 17).
42. Measured and Calculated (n; $\alpha$ ) Cross Sections of Cobalt. Calculations by Mann (49, 32).
43. Measured and Calculated (n;p) Cross Sections of Fe-56. Calculations by Mann (49, 27).
44. Calculated (n; $\alpha$ ) Cross Sections of Fe-56. Calculations by Mann (49).
45. Measured and Calculated (n;2n') and (n;3n') Cross Sections of Nb-93. Calculations by Young and Arthur using GNASH (48).
46. Present (solid curve) and Projected (dashed curve) Uncertainties in Total and Elastic- and Inelastic-scattering Cross Sections as a Function of Incident-neutron Energy.



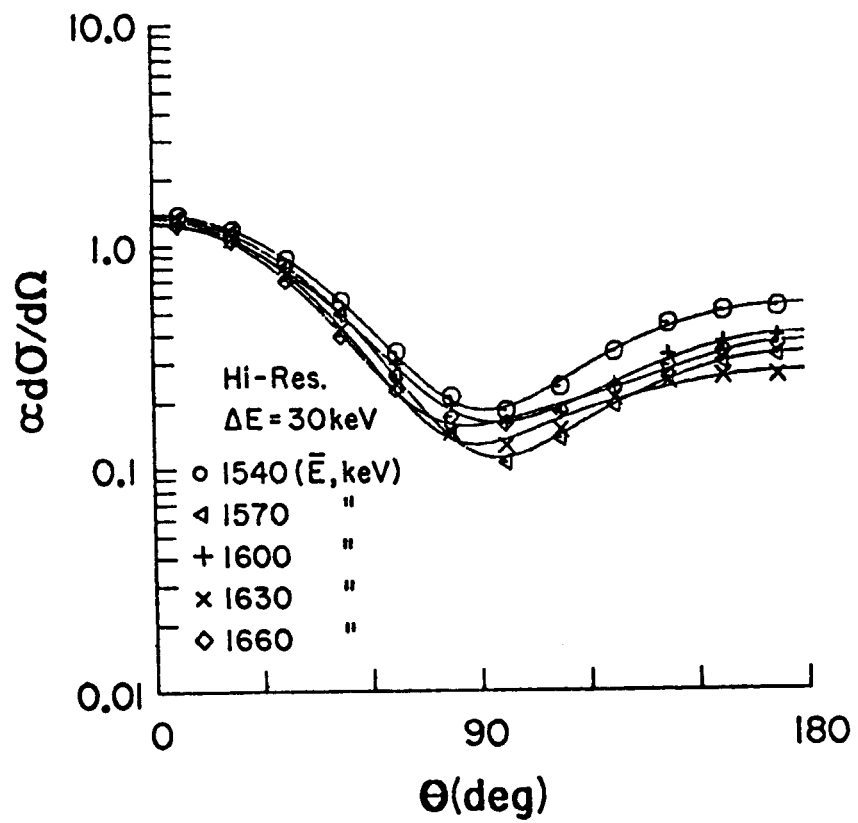


FIG. 4

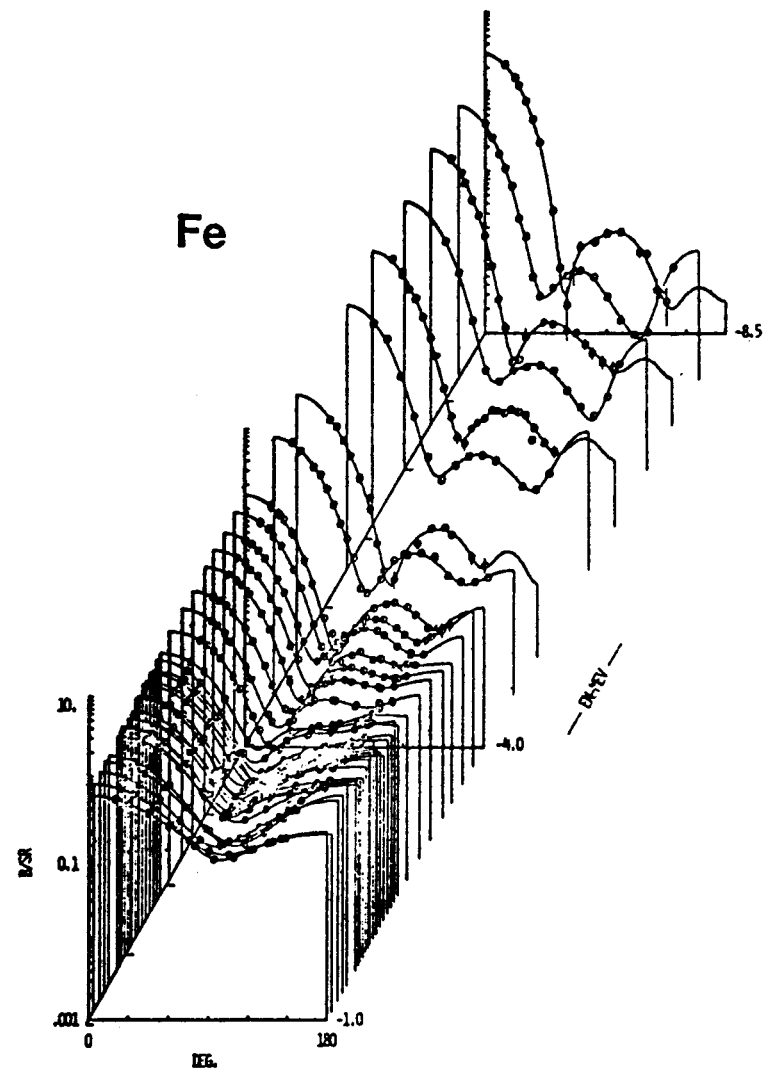


FIG. 5

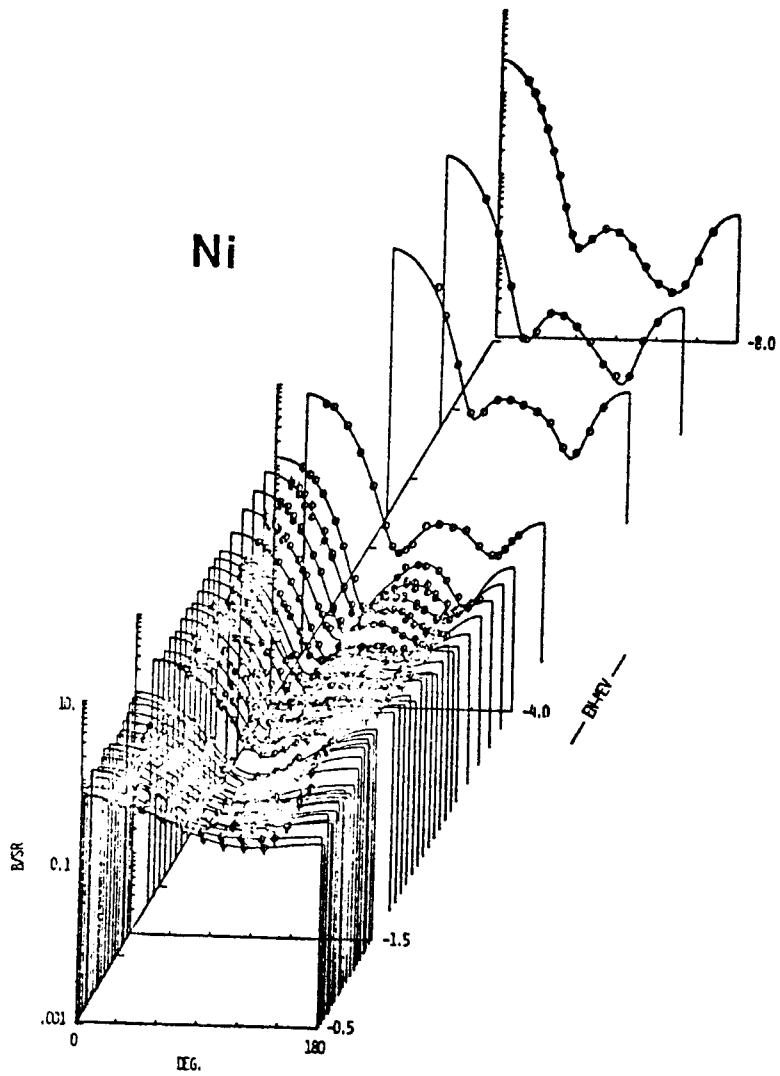


FIG. 6

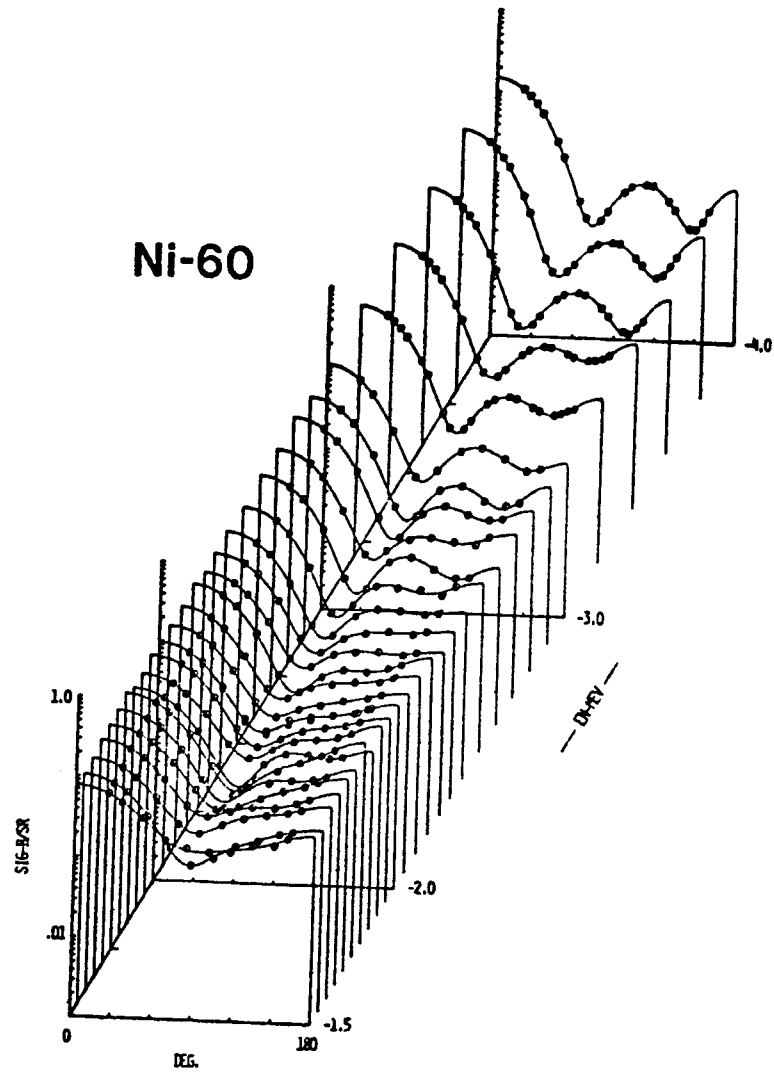


FIG. 7

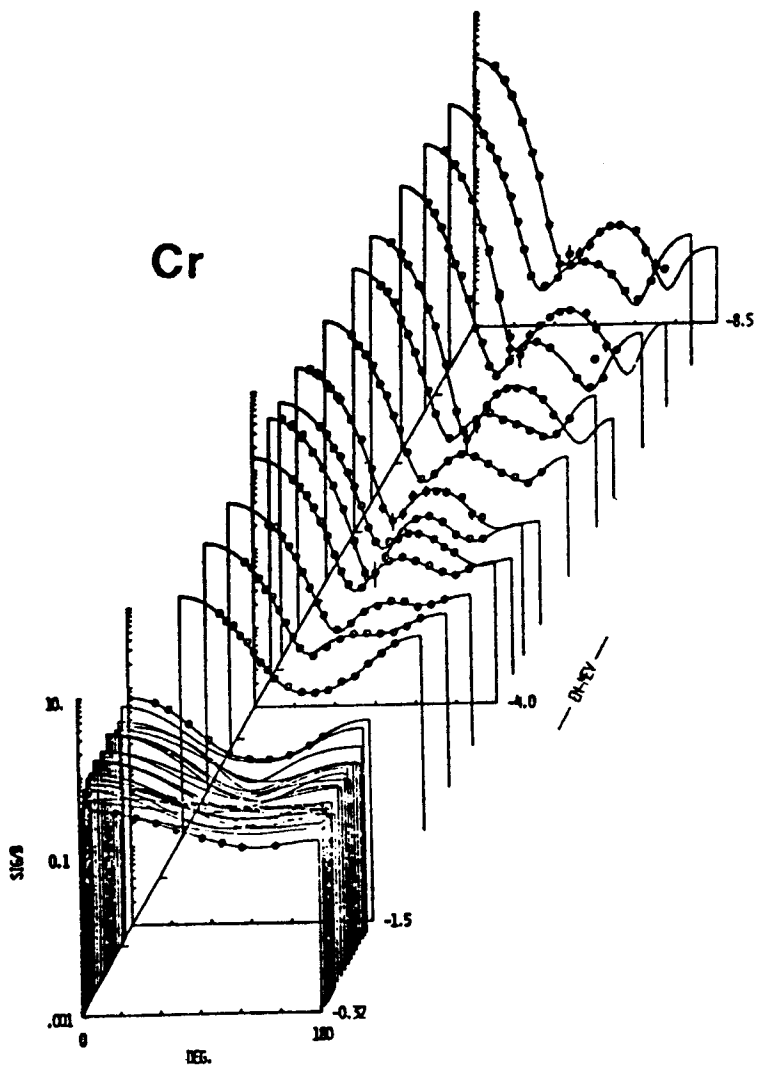


FIG. 8

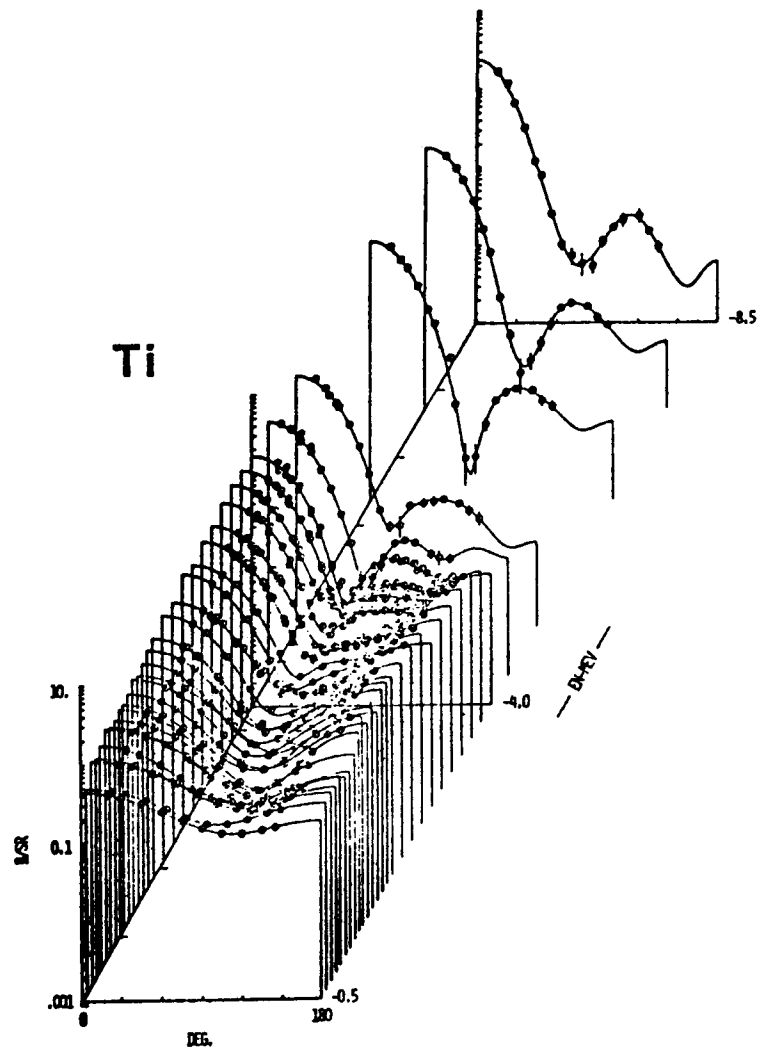


FIG. 9

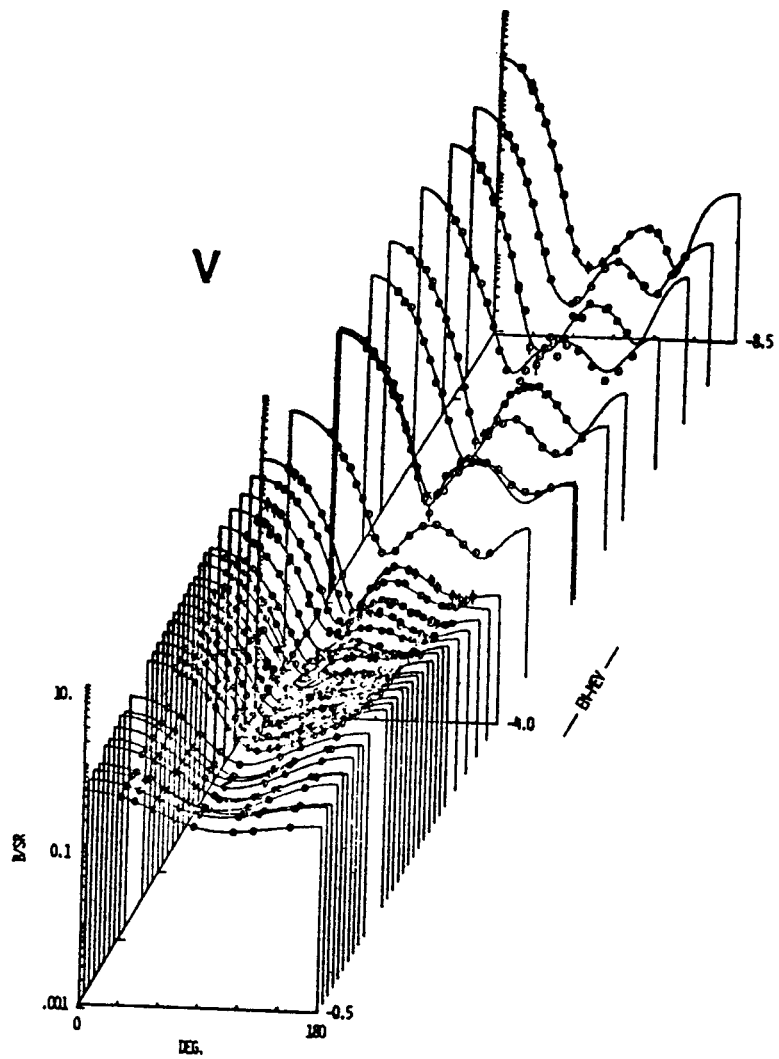


FIG. 10

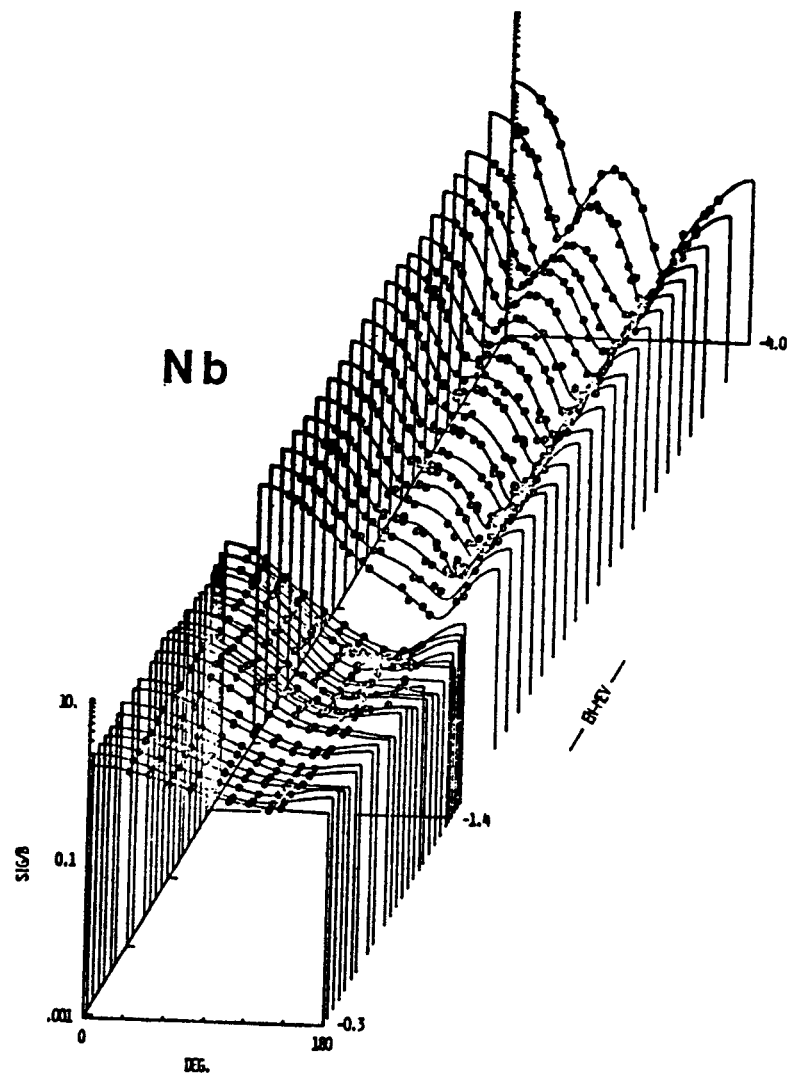


FIG. 11

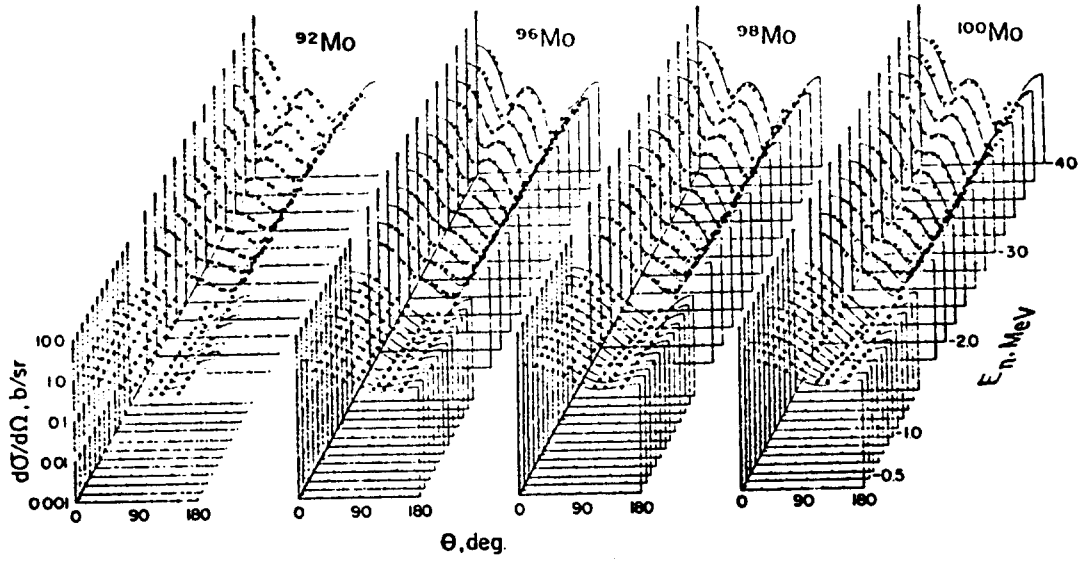


FIG. 12

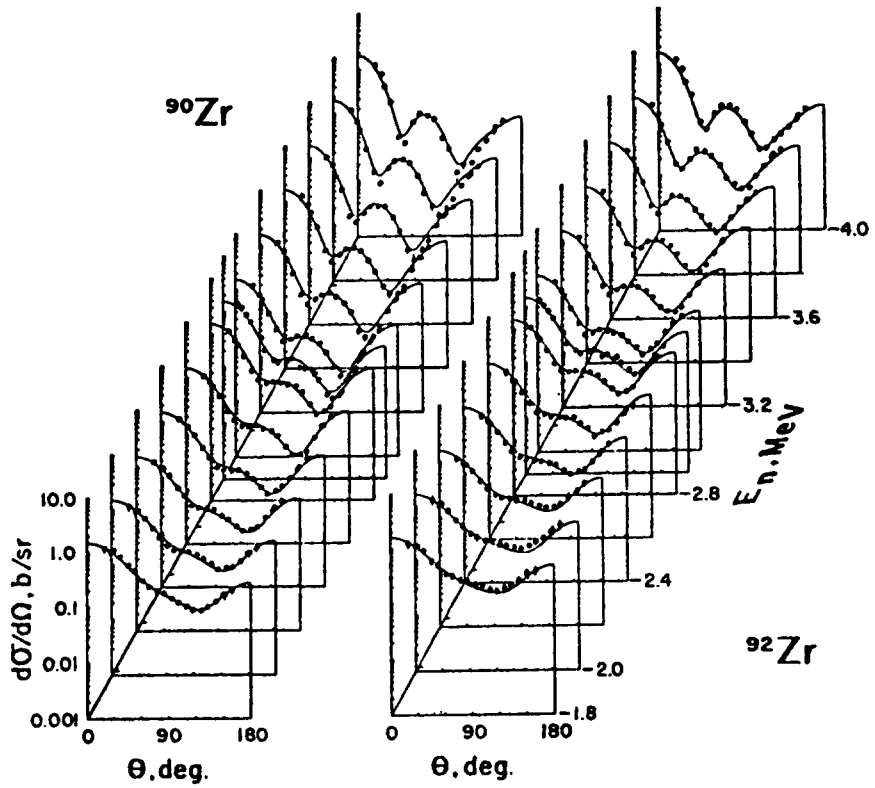


FIG. 13

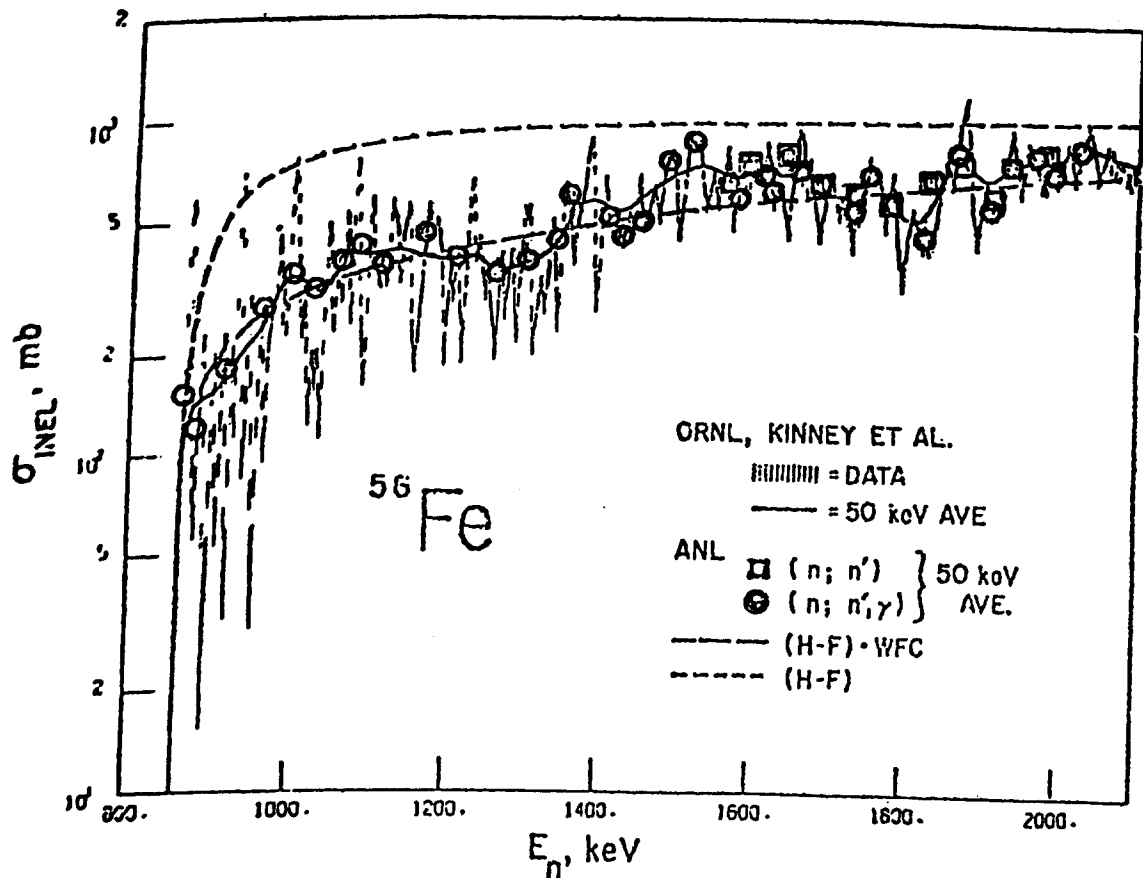


FIG. 14

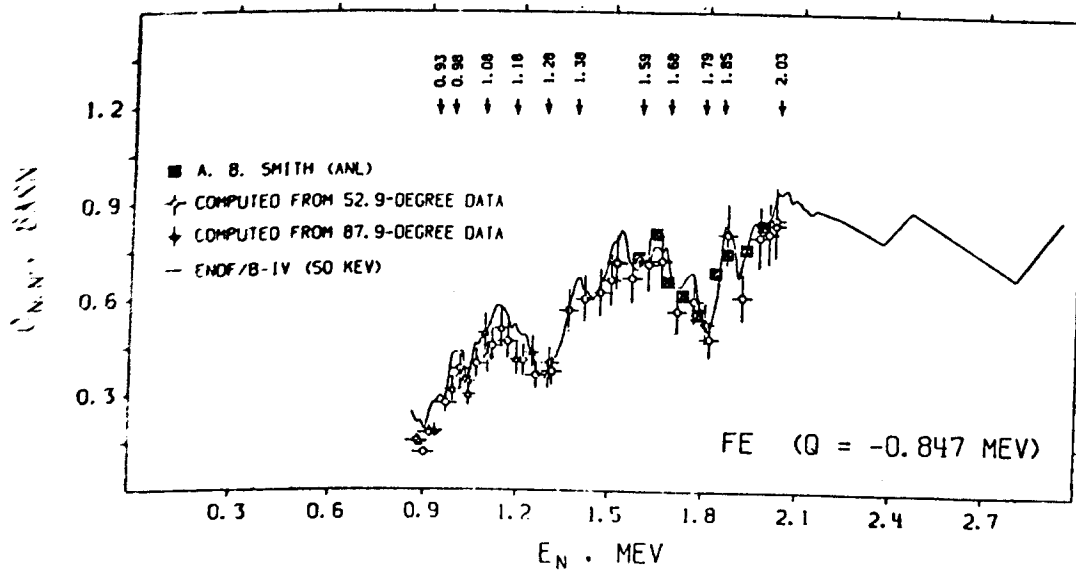


FIG. 15

FIG. 16

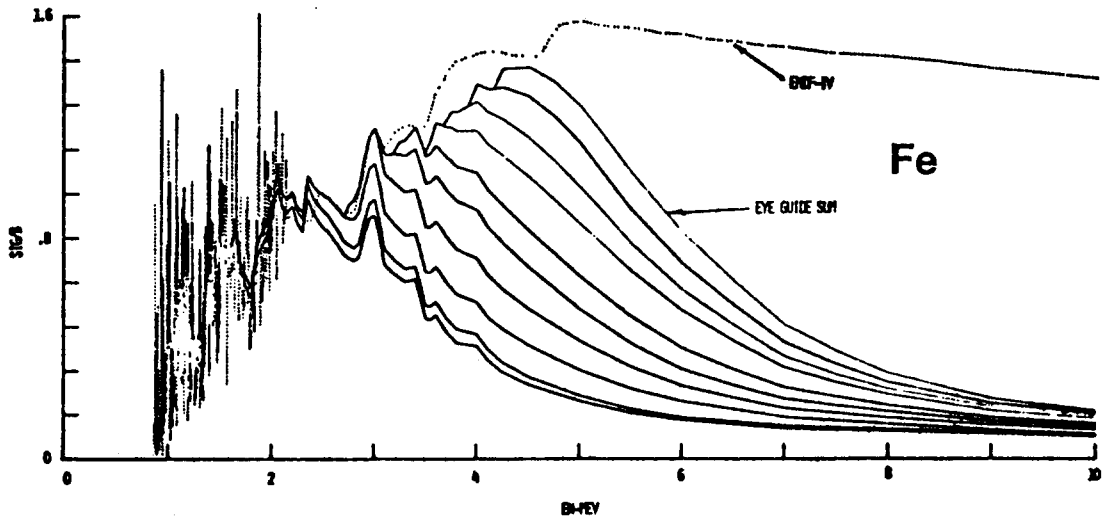
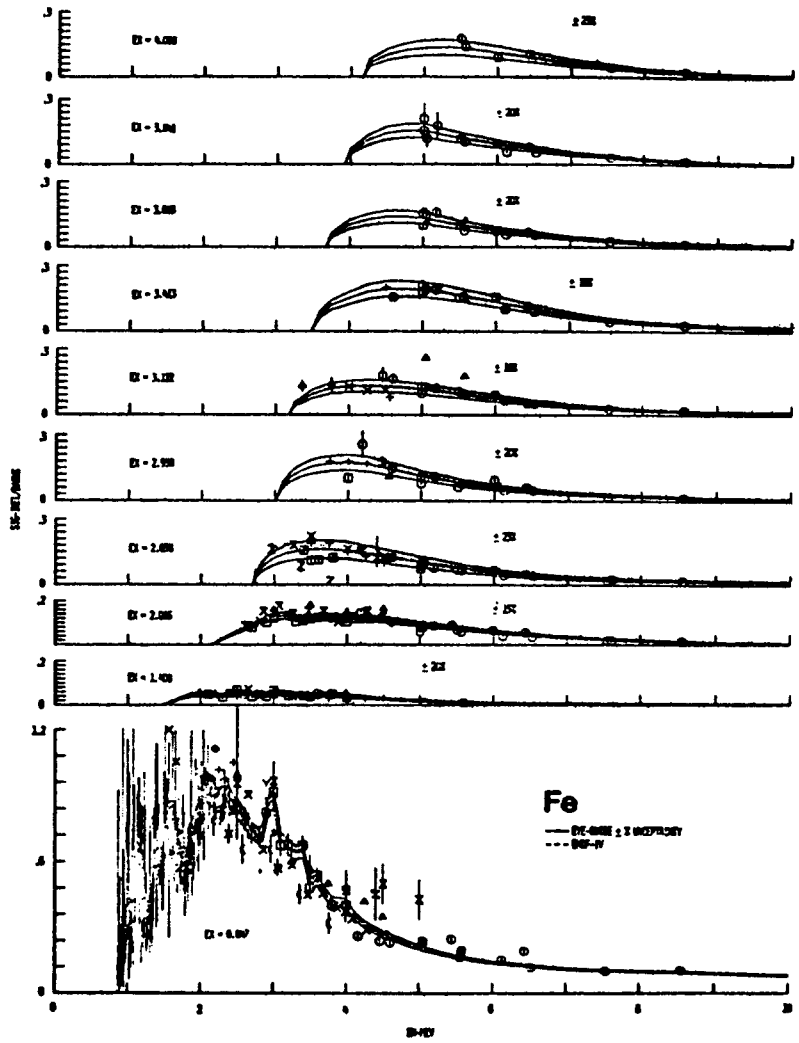


FIG. 17

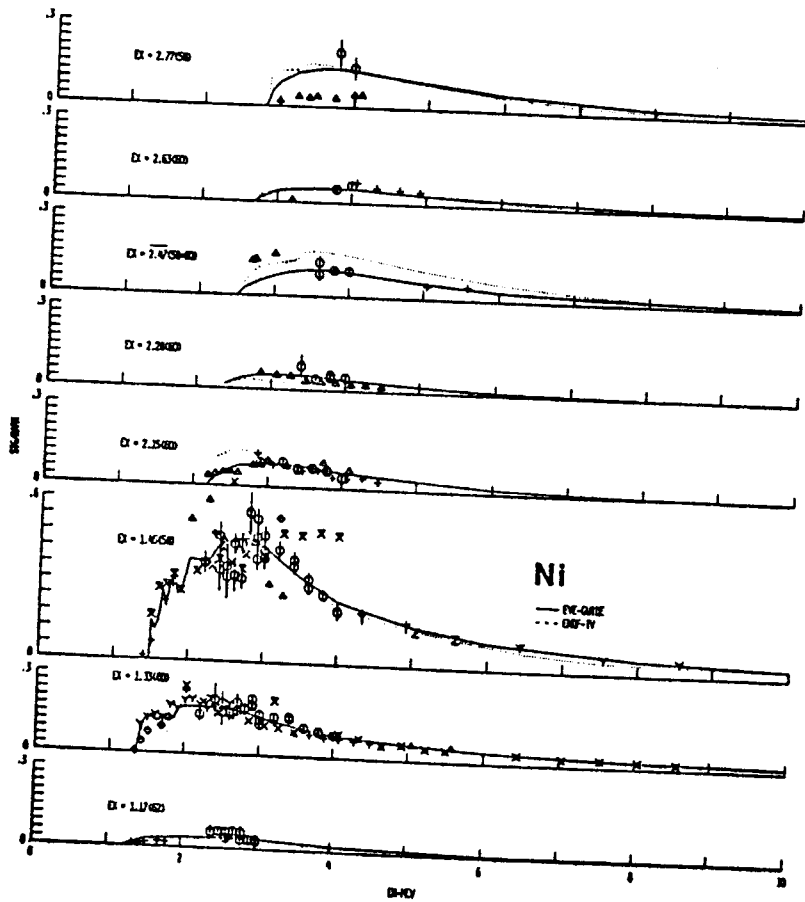


FIG. 18

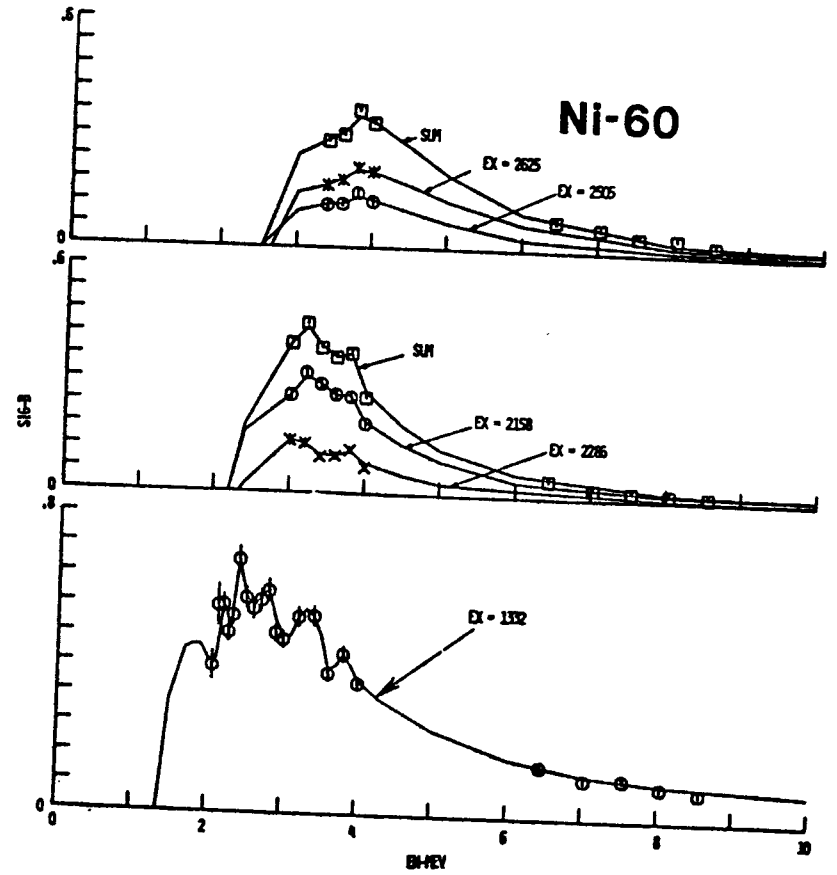


FIG. 19

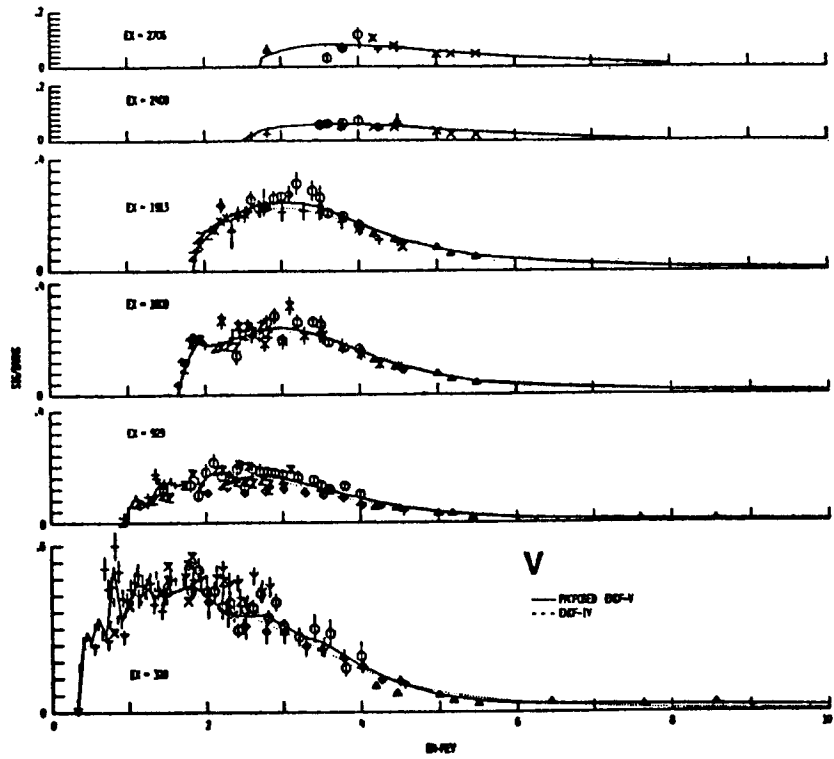


FIG. 20

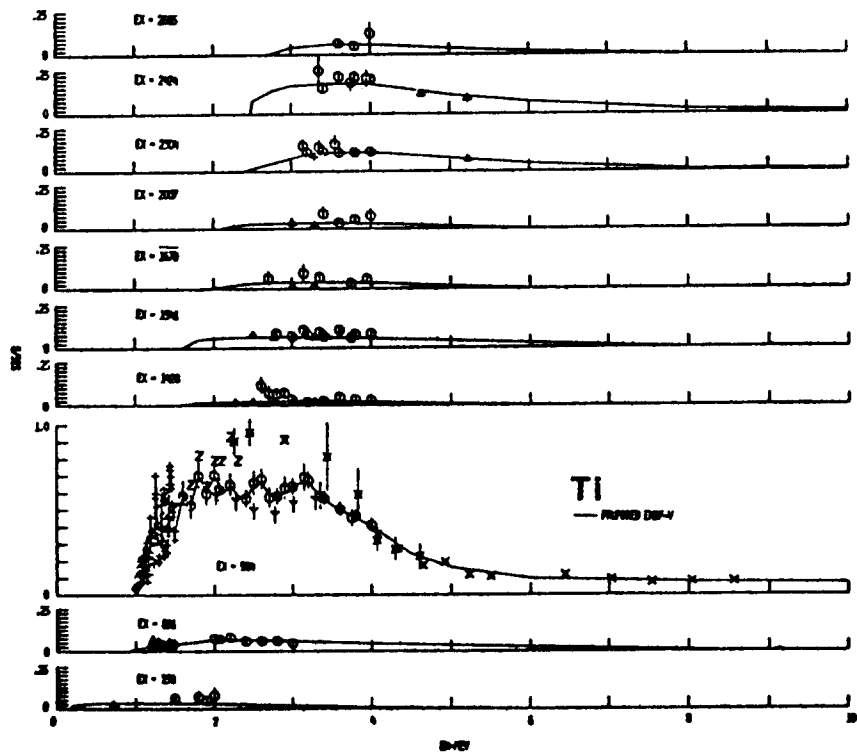


FIG. 21



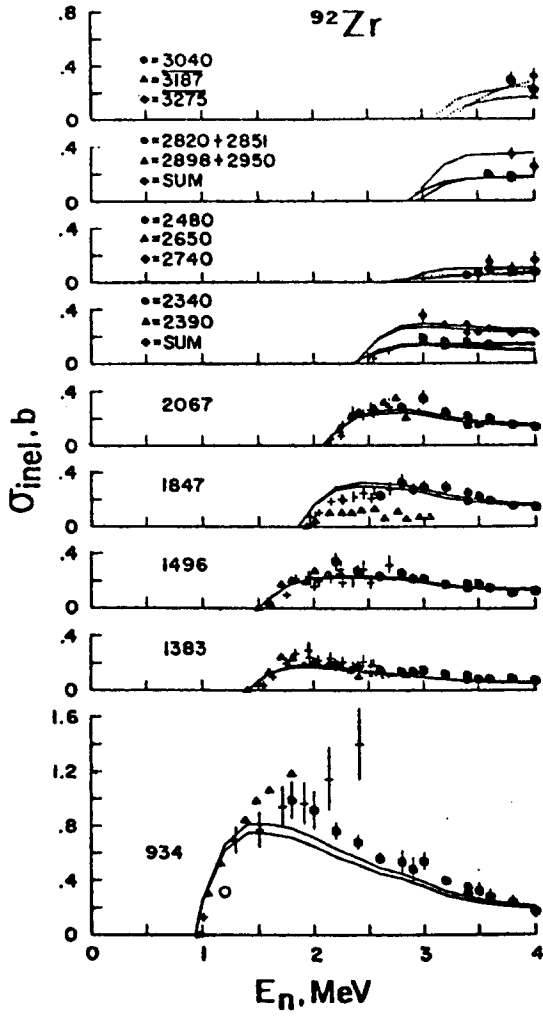


FIG. 24

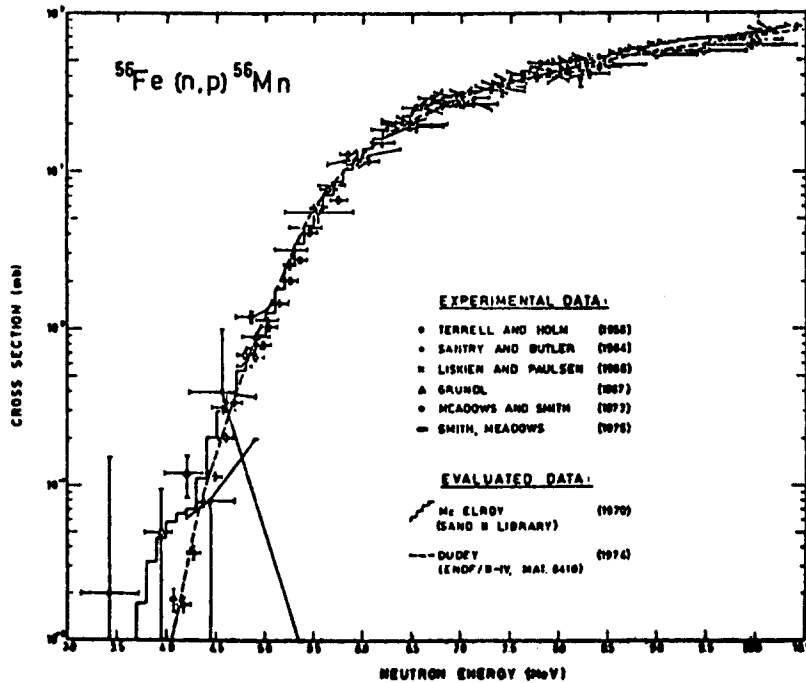
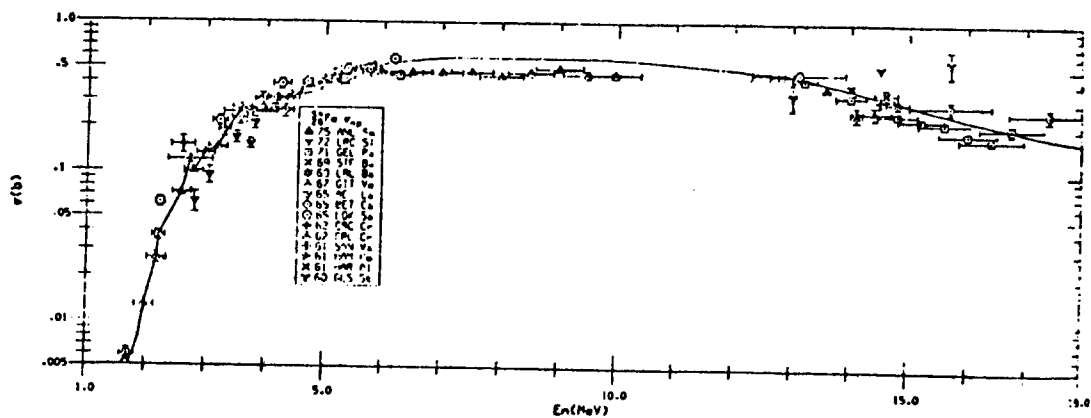
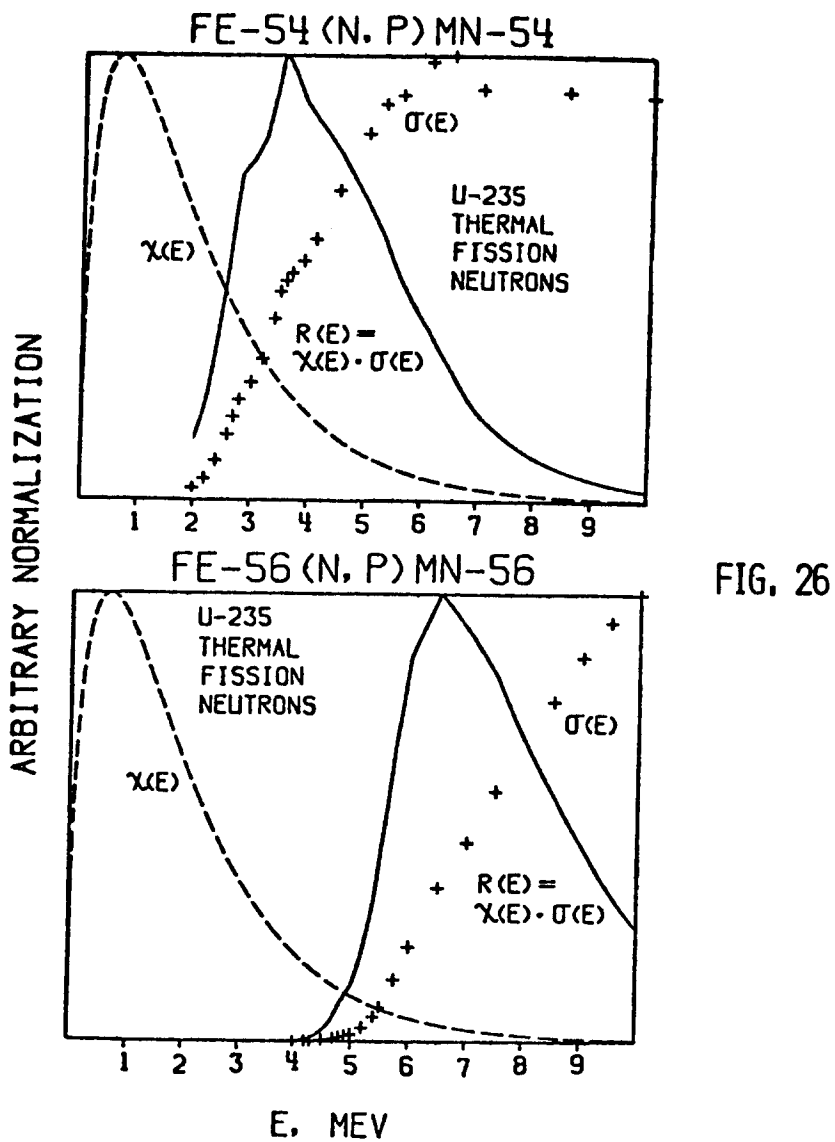


FIG. 25



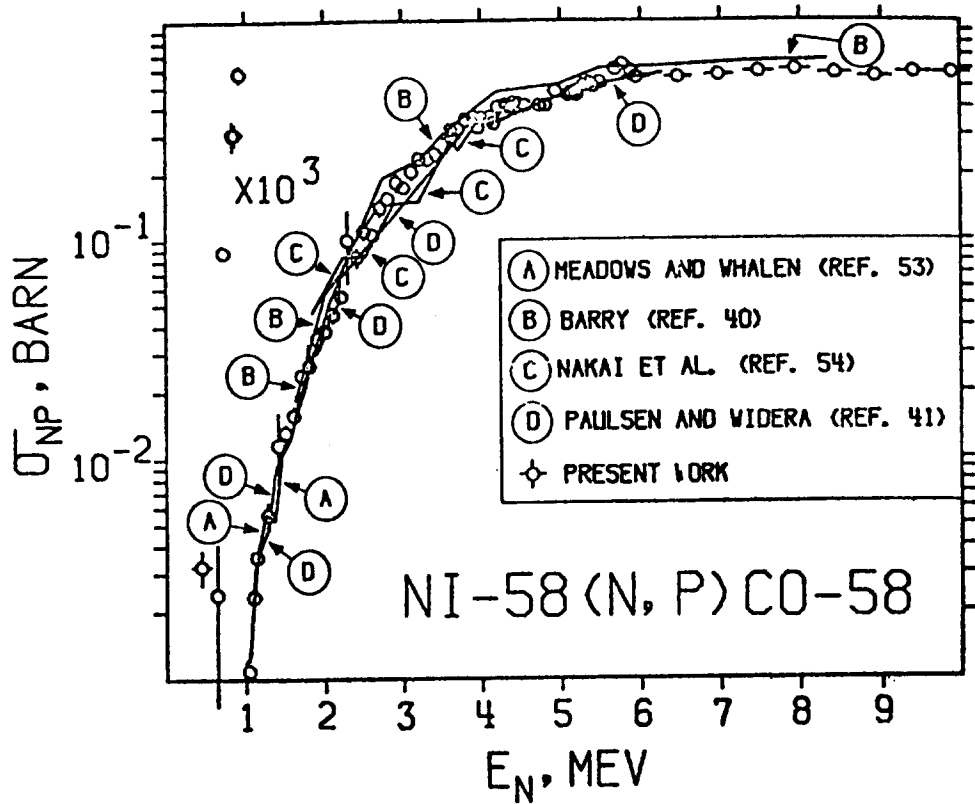


FIG. 28

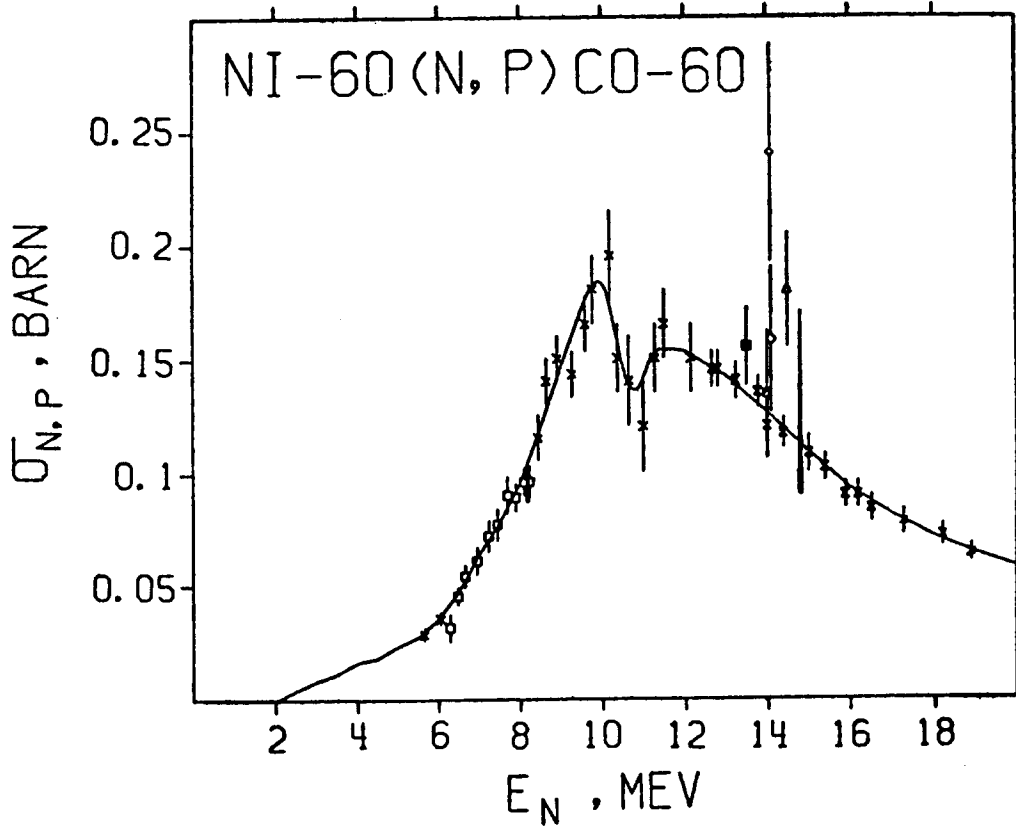


FIG. 29

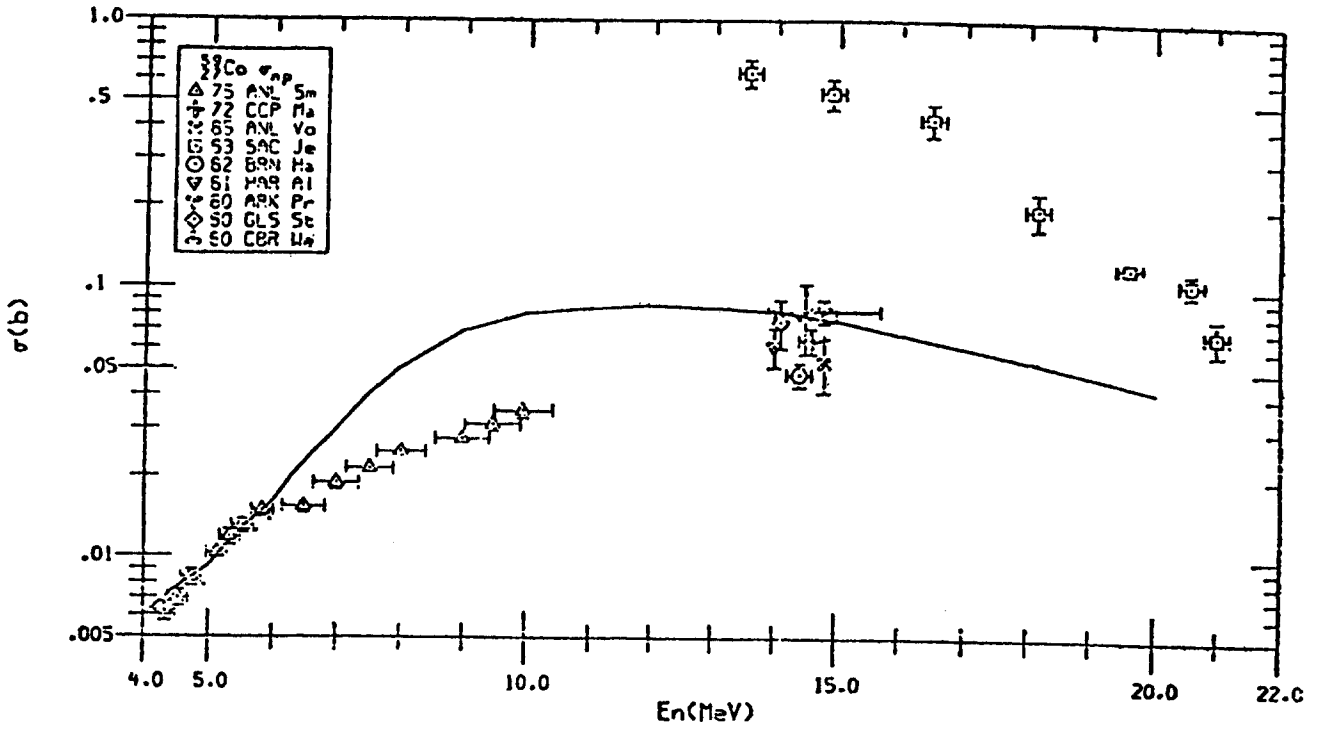


FIG. 30

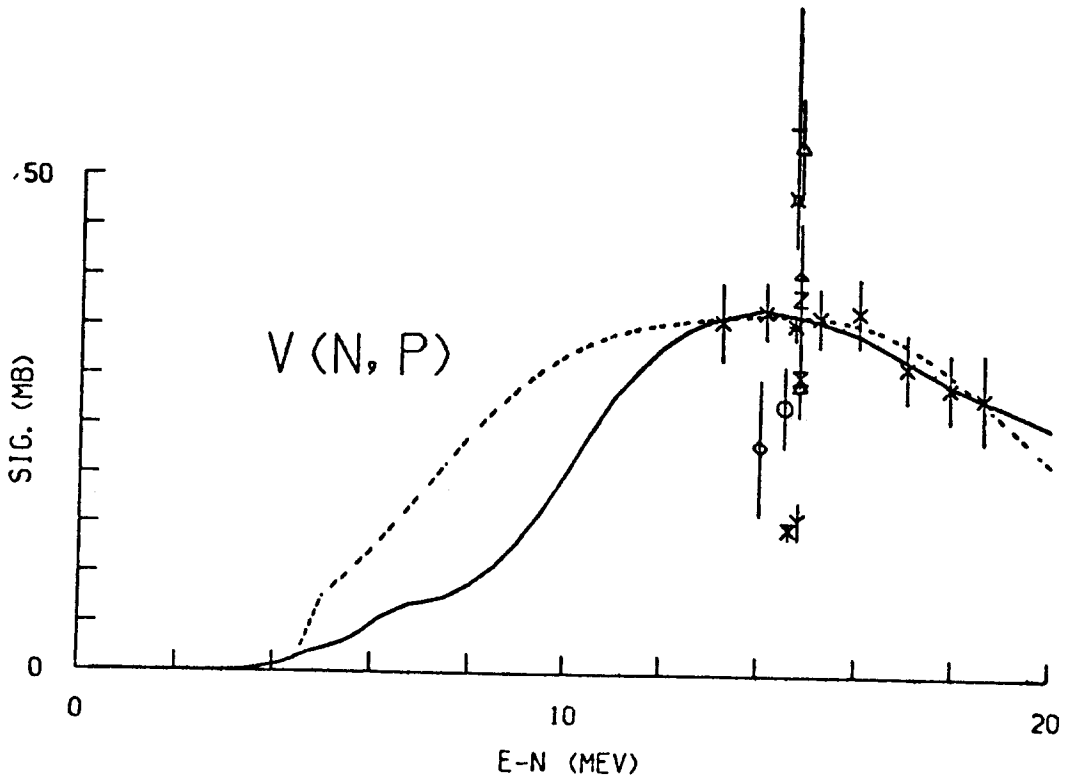
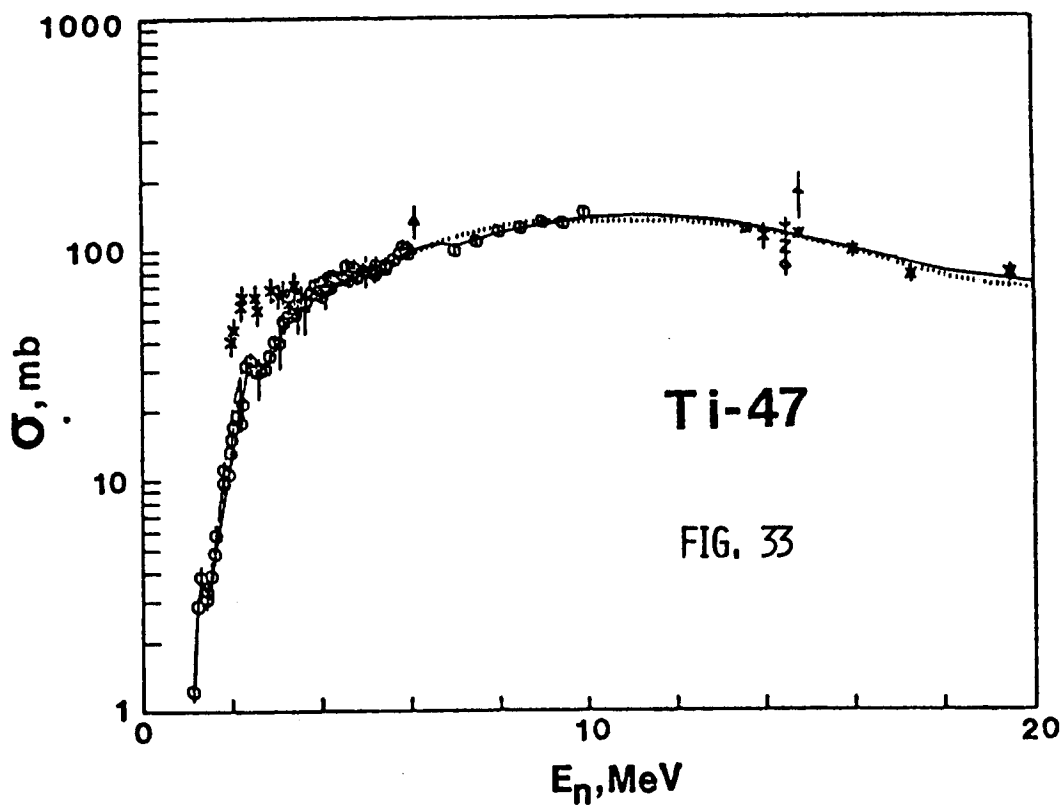
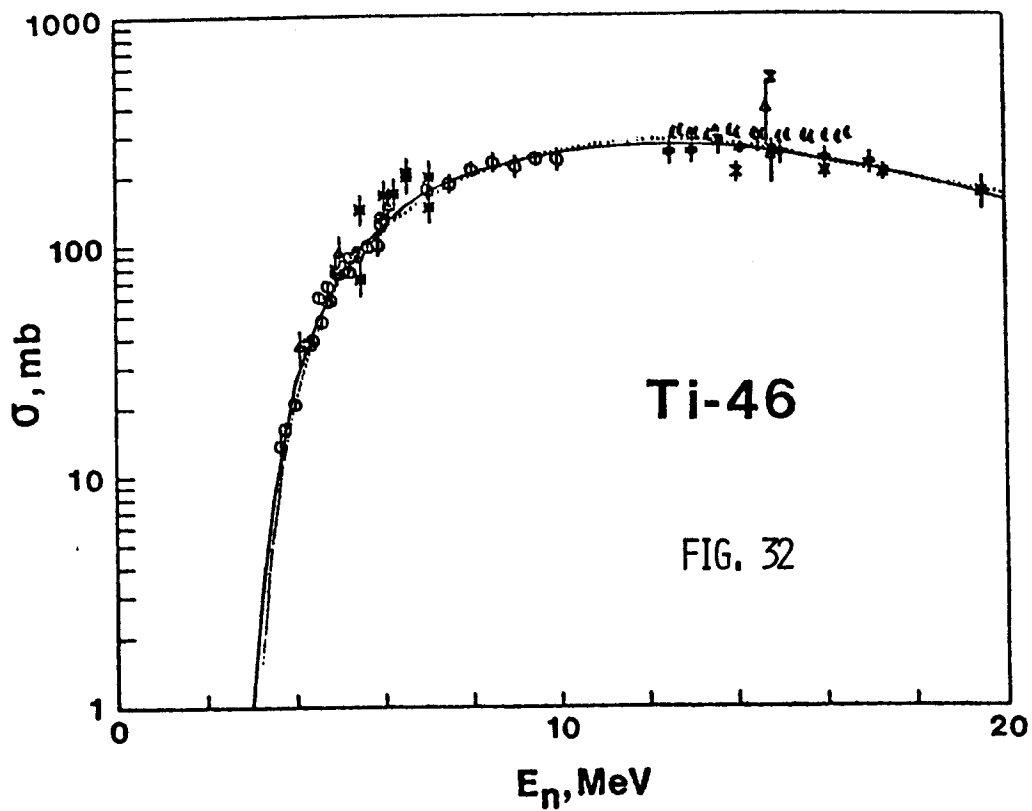


FIG. 31



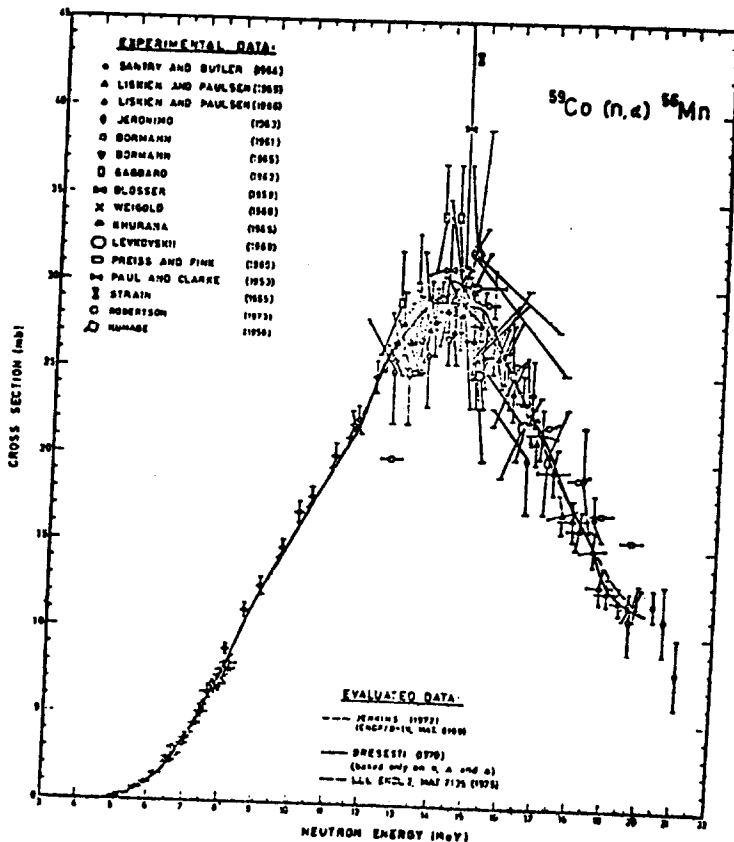
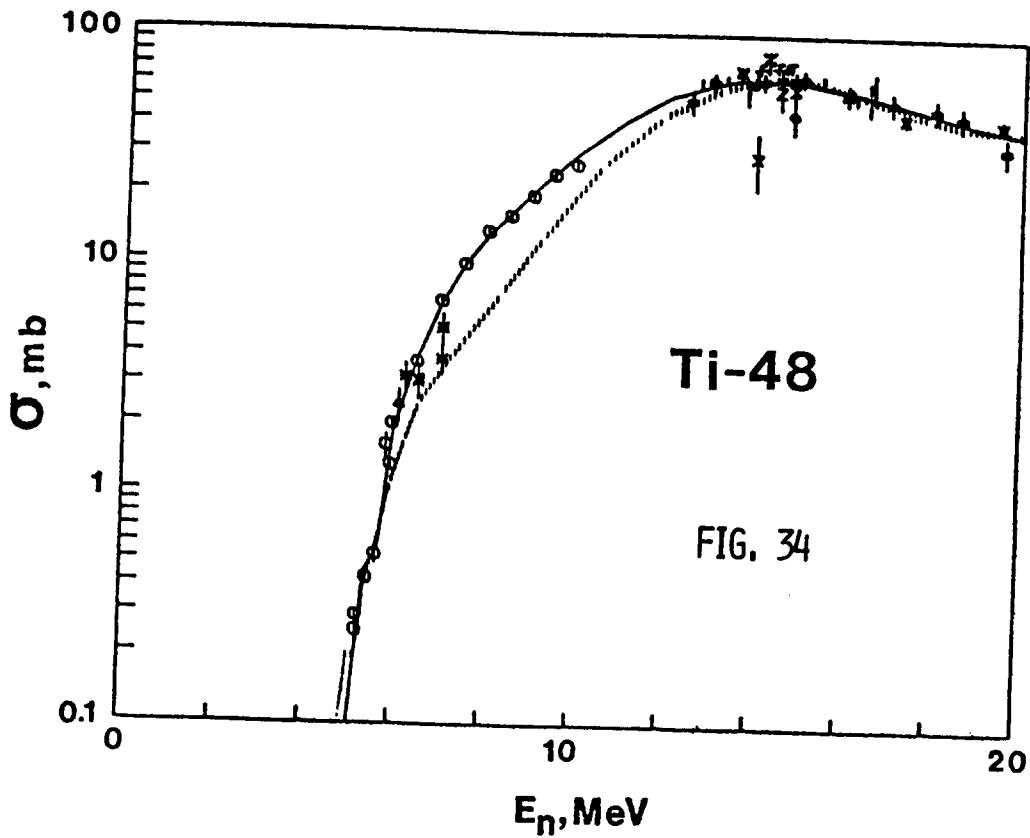


FIG. 35

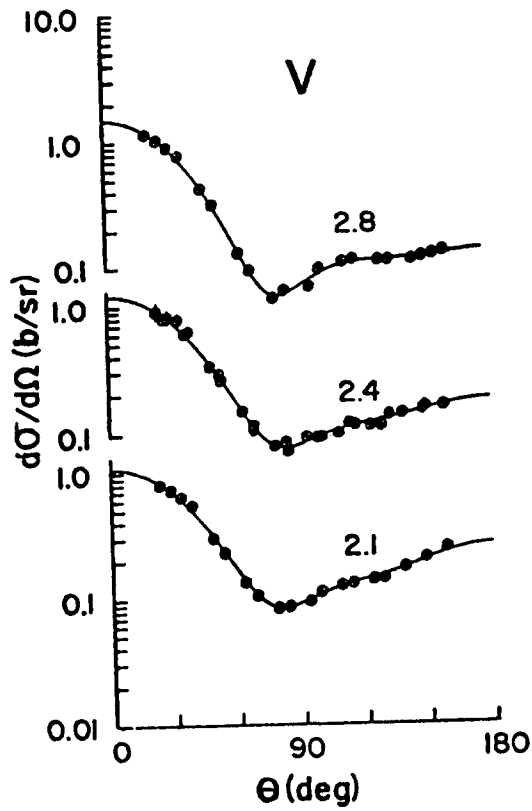
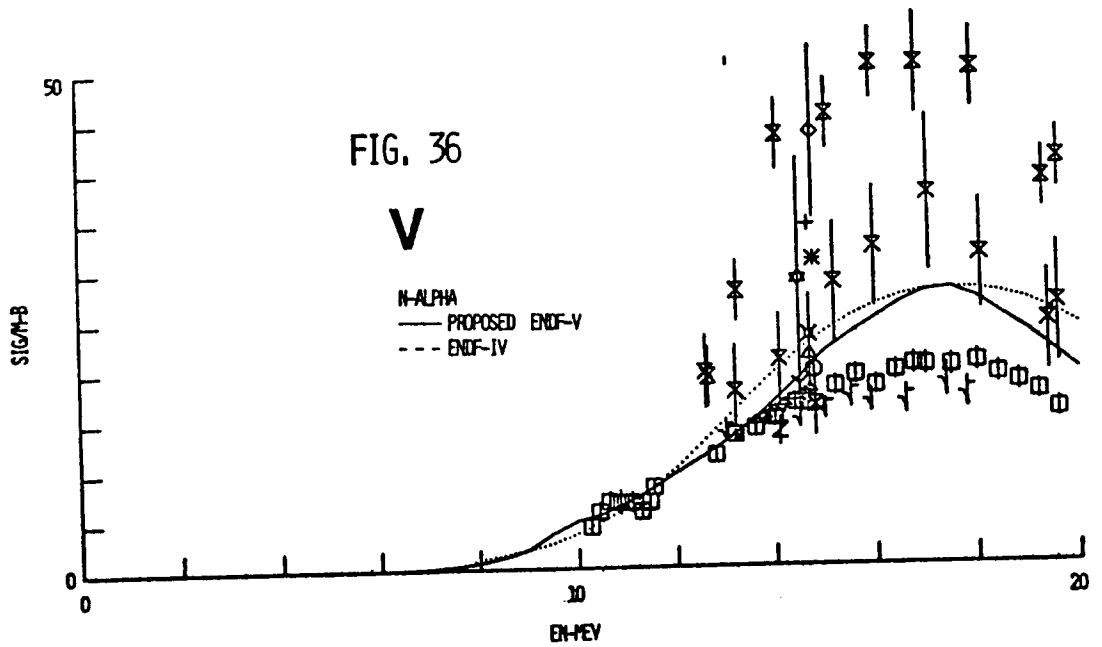


FIG. 37

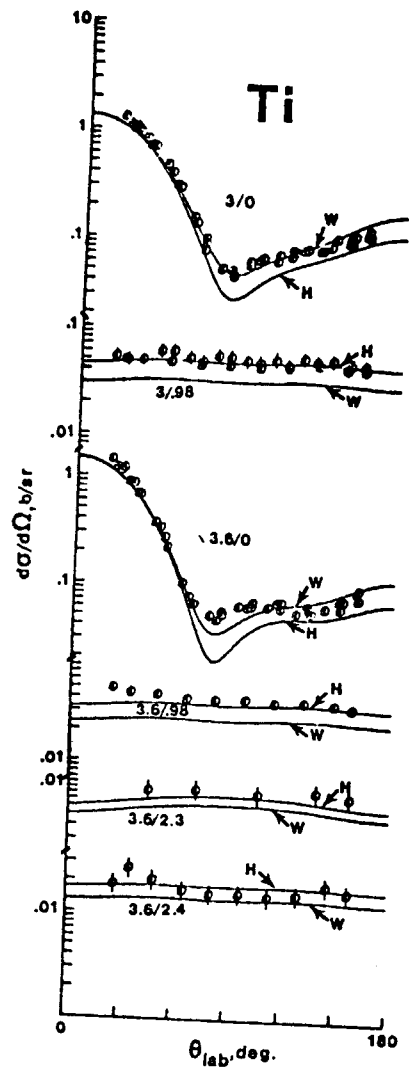


FIG. 38

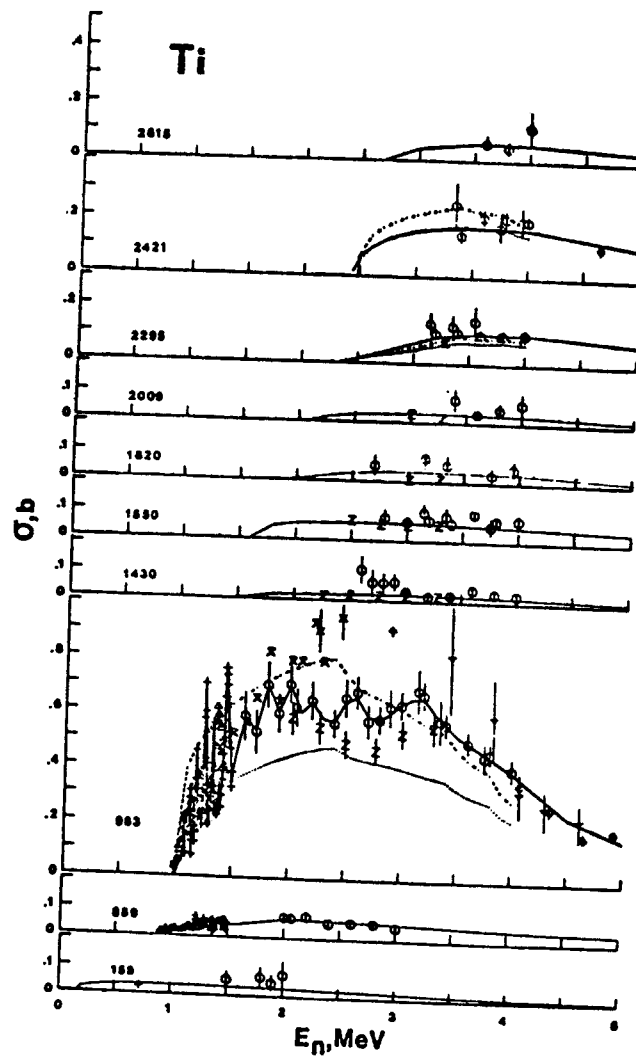


FIG. 39

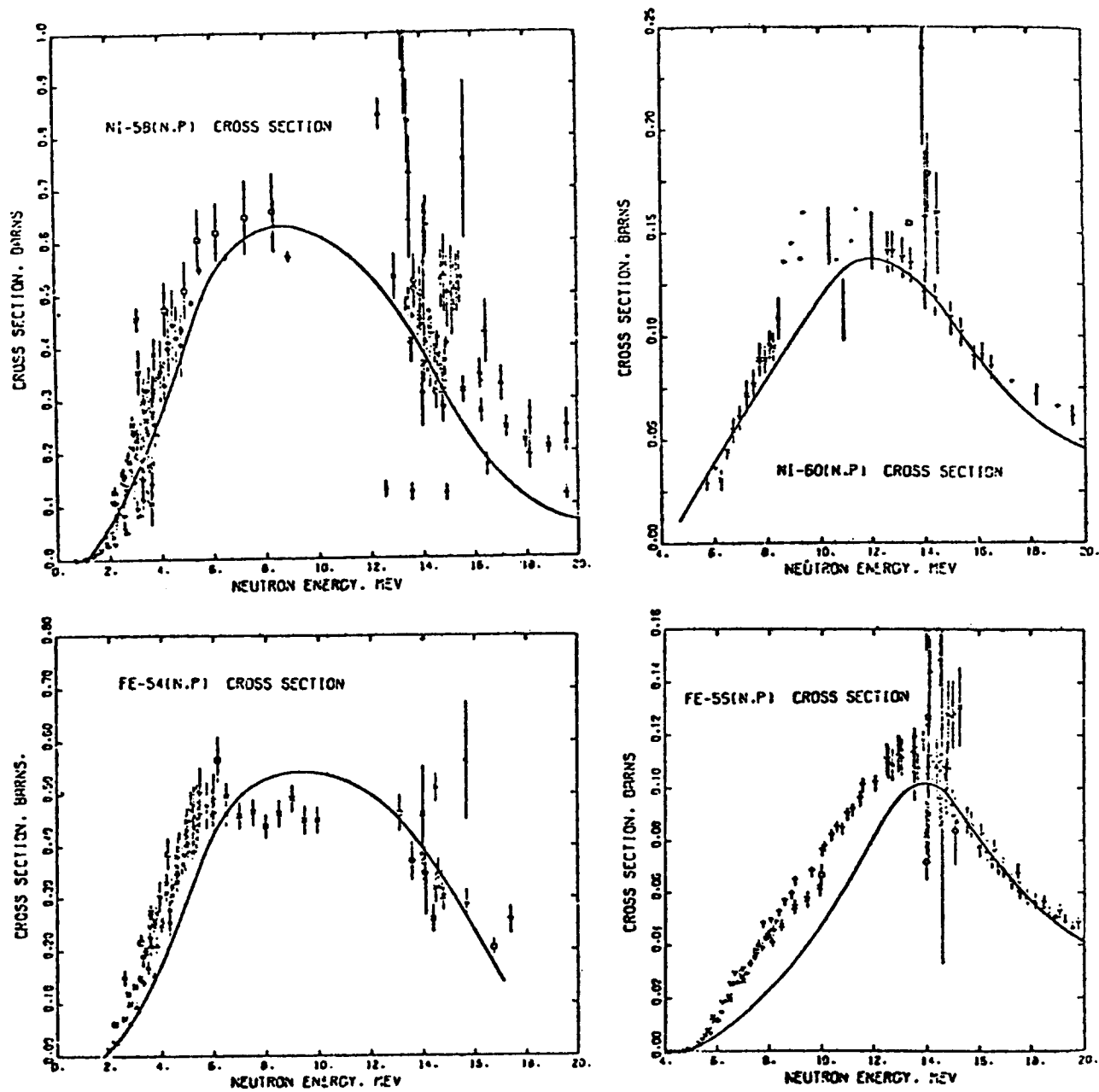
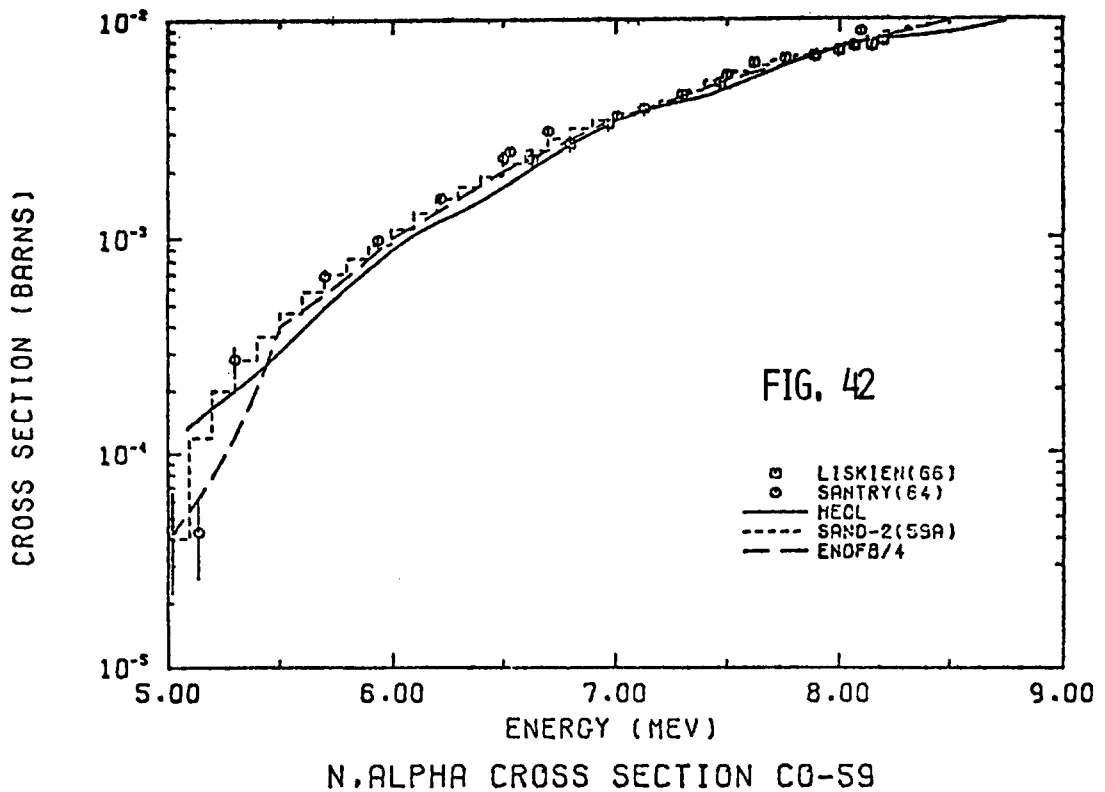
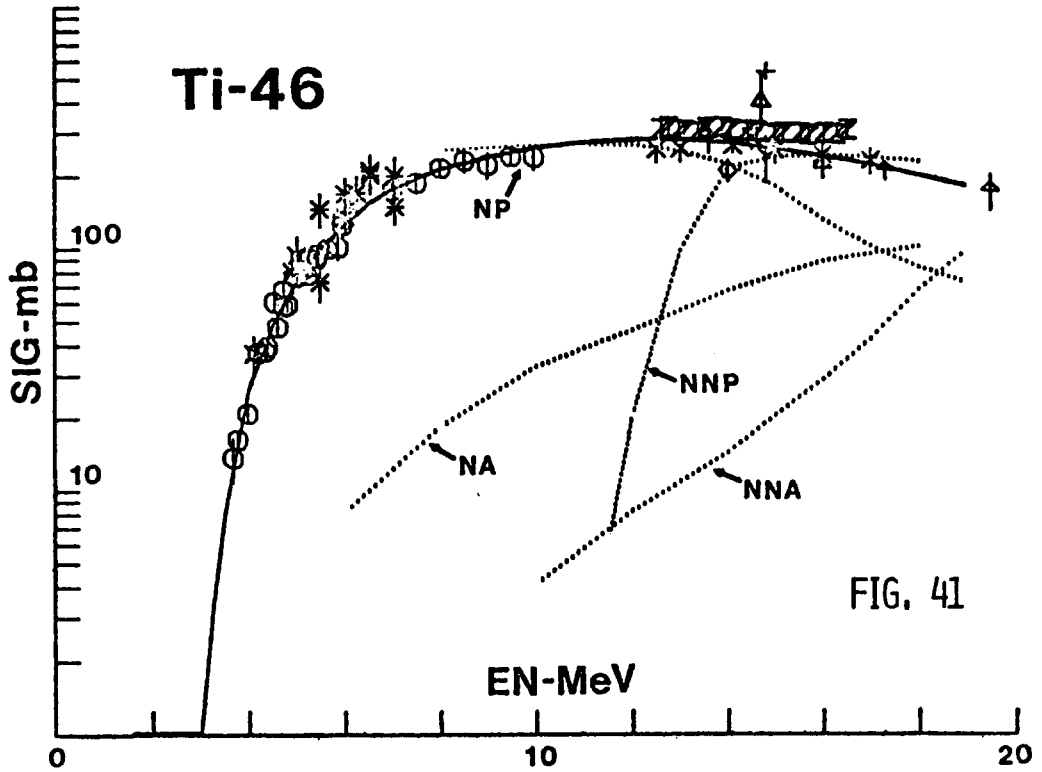
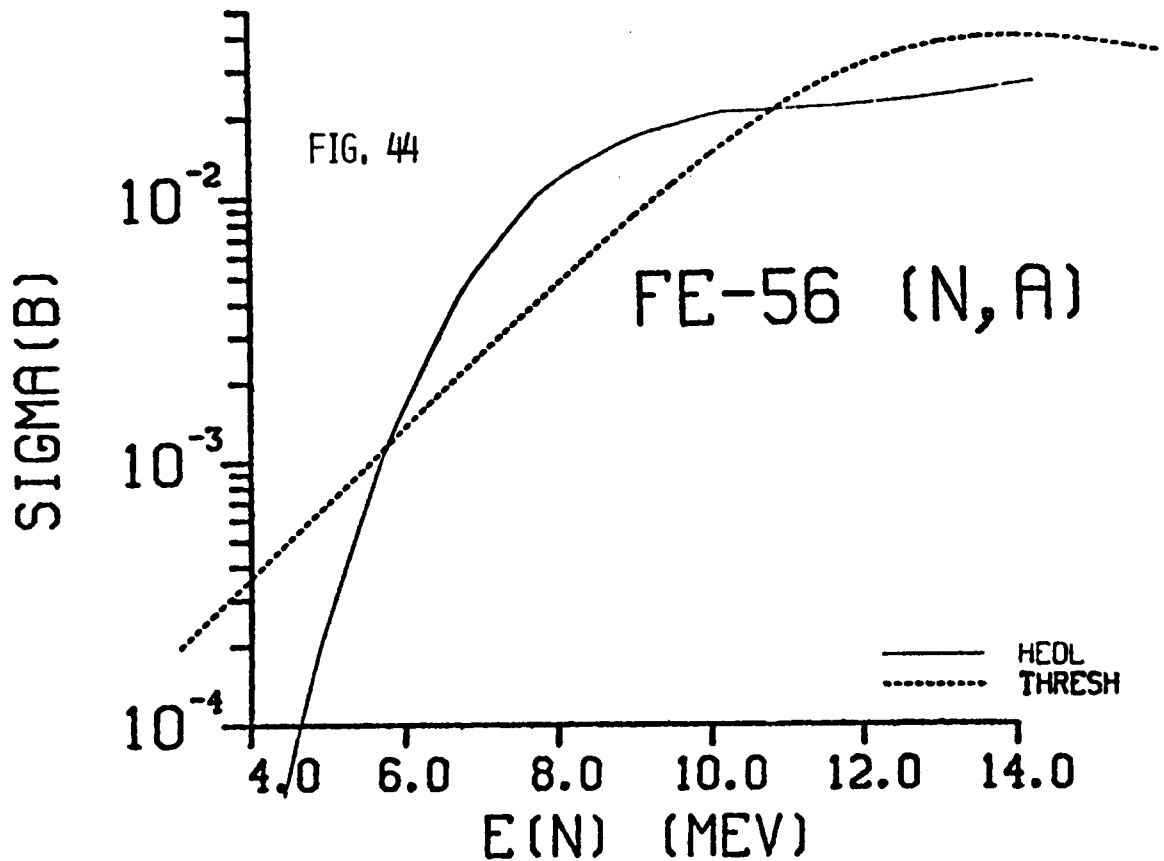
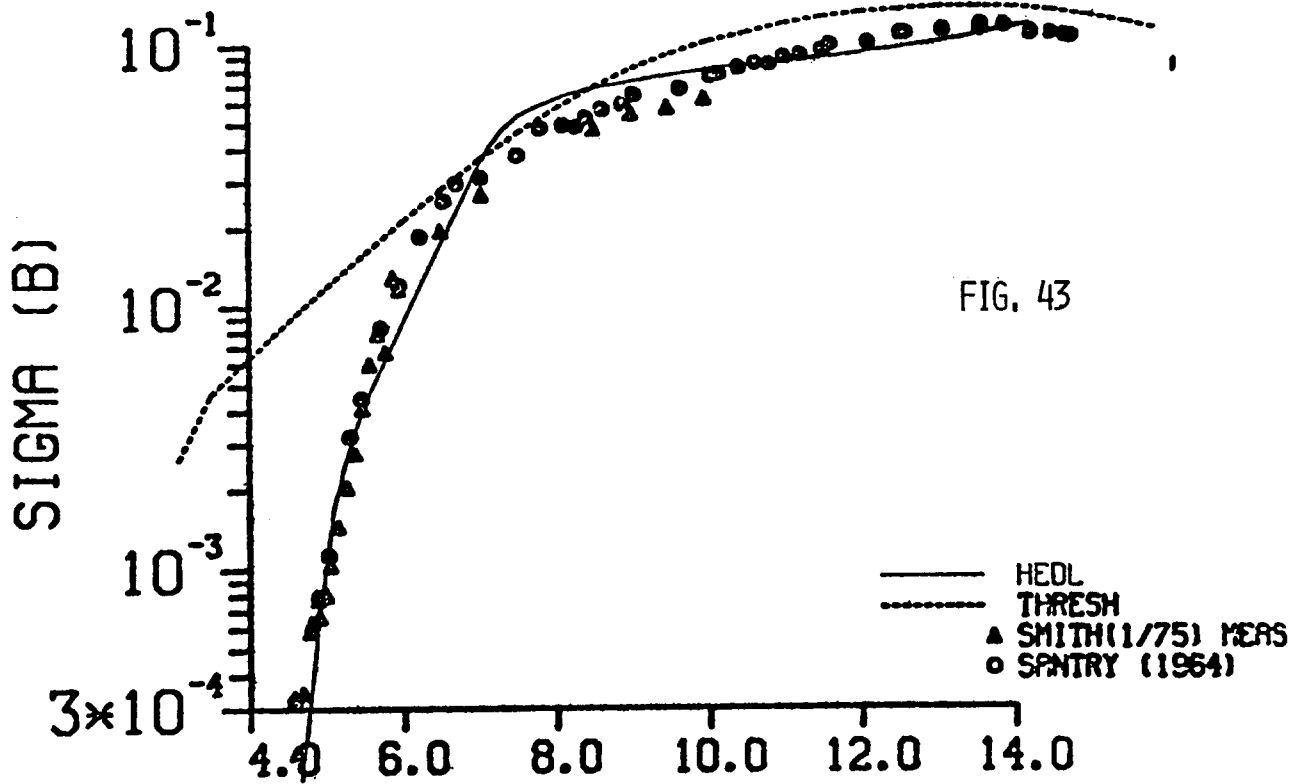


FIG. 40



## FE56 (N, P)



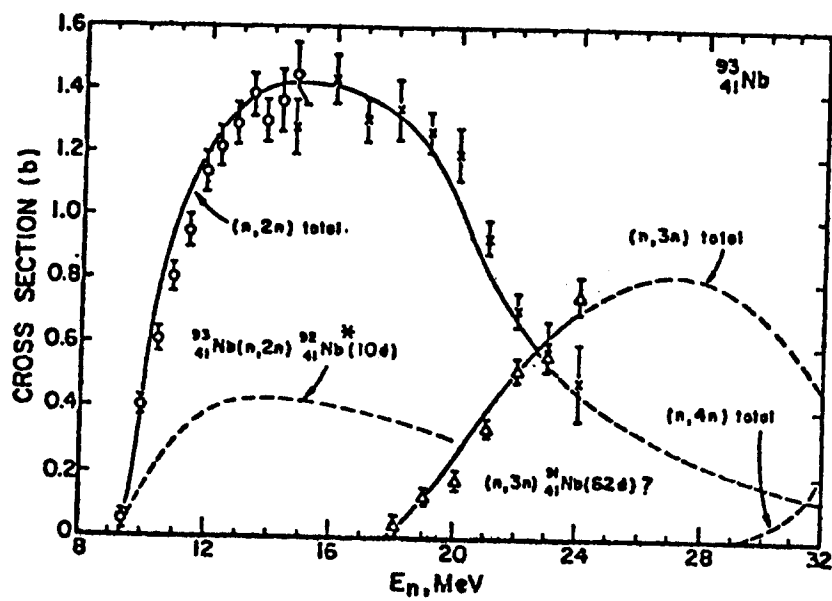


FIG. 45

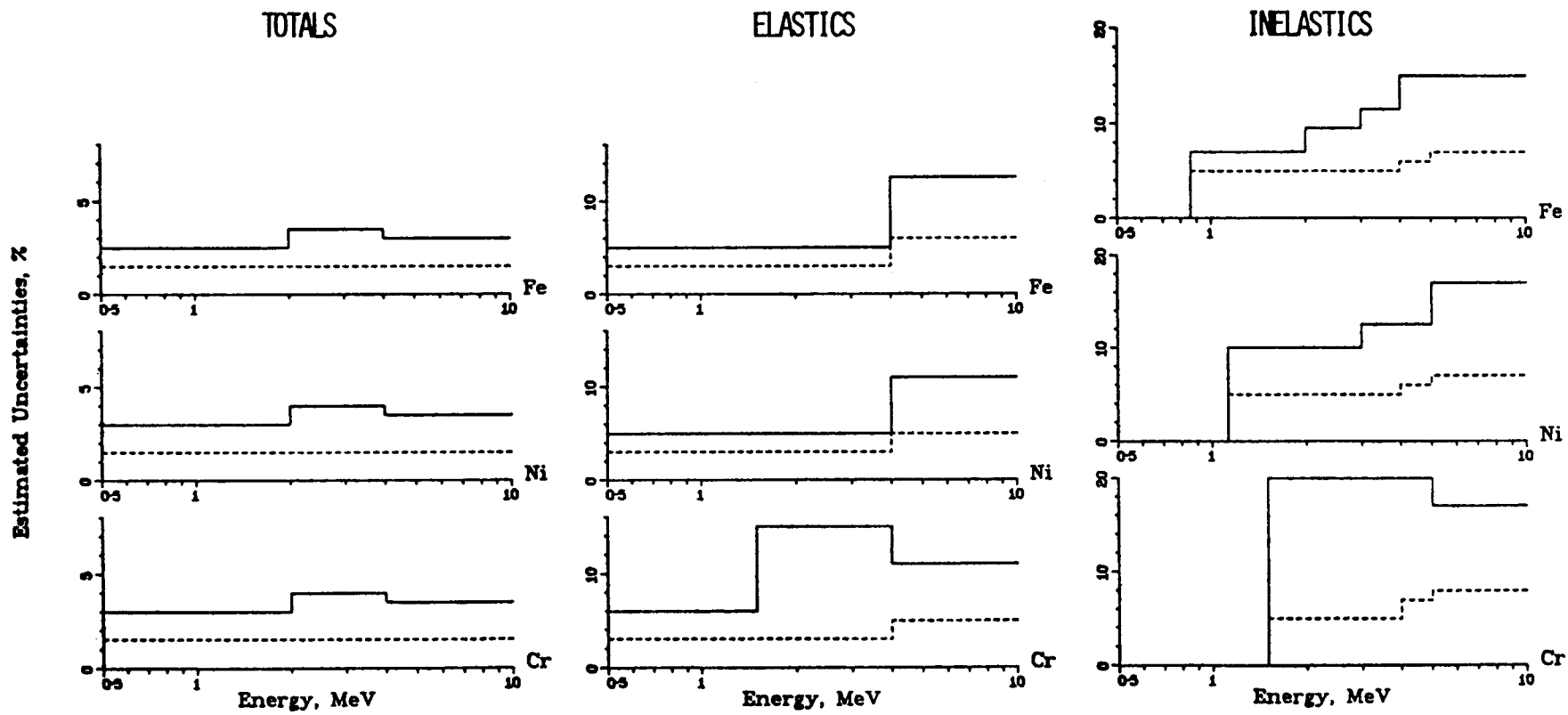


FIG. 46